The Motion of a Pushed, Sliding Object
Part 2: Contact Friction

M. A. Peshkin and A. C. Sanderson

CMU-RI-TR-86-7

The Robotics Institute
Carnegie-Mellon University
Pittsburgh, Pennsylvania 15213

April 1986

This work was supported by a grant from Xerox Corporation, and by the Robotics Institute, Carnegie-Mellon University.

Table of Contents

List of Figures

Abstract

The physics of motion of a sliding object can be used to plan sensorless robot manipulation strategies based on sliding. Prediction of a sliding object's motion is difficult because the object's distribution of support on the surface, and the resulting frictional forces, are in general unknown. We describe a new approach to the analysis of sliding motion, which finds the set of object motions for *all* distributions of support. The analysis includes contact friction between the pusher and pushed object, as well as sliding friction between the pushed object and the surface it slides on. To demonstrate the use of our results, we find the distance a polygonal object must be pushed by a fence to assure alignment of an edge of the object with the fence. We also analyze the motion of a sliding disk as it is pushed aside by the corner of an object in linear motion. Finally, we consider a sensorless manipulation strategy based on "herding" a sliding disk toward a central goal by moving a robot finger in a decreasing spiral about the goal. The optimal spiral is constructed, and its performance discussed.

1. Background

1.1. Motivation

A discussion of previous work on sliding, and of the motivation for this work, may be found in an earlier report "The Motion of a Pushed, Sliding Object, part 1: sliding friction" [4].

1.2. The Center of Rotation

An object sliding on a table has three degrees of freedom. Its position may be specified by the (x,y) displacement and angle θ of a coordinate frame fixed in the object relative to a coordinate frame fixed in the table. The object's instantaneous motion can be described as infinitesimal changes in the displacements and rotation.

Here we will treat the object as a two-dimensional rigid body, since we are only concerned with the object's interaction with the table it is sliding on. All pushing forces will be restricted to lie in the plane of the table as well. The results may be applied to three-dimensional objects, as long as the vertical component of the pushing force is negligible, and as long as the point of contact is near the table.

When an object is being pushed, in the general case there is only one point of contact between the object and the pusher. The contact may be where the leading edge of a pushing fence touches a corner of the object (figure 1-1), or it may be where a pushing point touches an edge of the object (figure 1-2.) The analysis presented here applies to either case. In many figures (e.g., figure 2-2) just an 'edge' will be drawn, which may be the pushed edge of the object or the front edge of a fence.

The pusher is assumed to move along a predetermined path in the plane of the table (that is, it is under position control). The object retains two degrees of freedom, with the third degree of freedom of its motion fixed by the requirement to maintain contact between the pusher and the object.

These two degrees of freedom are most conveniently expressed as the coordinates of a point in the plane called the *center of rotation* (COR.) Any infinitesimal motion of the object can be expressed as a rotation $\delta\theta$ about some COR, chosen so that the infinitesimal motion of each point $\vec{w}$ of the object is perpendicular to the vector from the COR to the point $\vec{w}$. If the object is a disk, and the motion it performs is pure rotation in place, the COR is at the center of the disk. Motions we might describe as "mostly translation" correspond to CORs far from the point of contact. In the extreme case, pure translations occur when the COR is at infinity.

The weight of an object is supported by a collection of contact points between the object and the

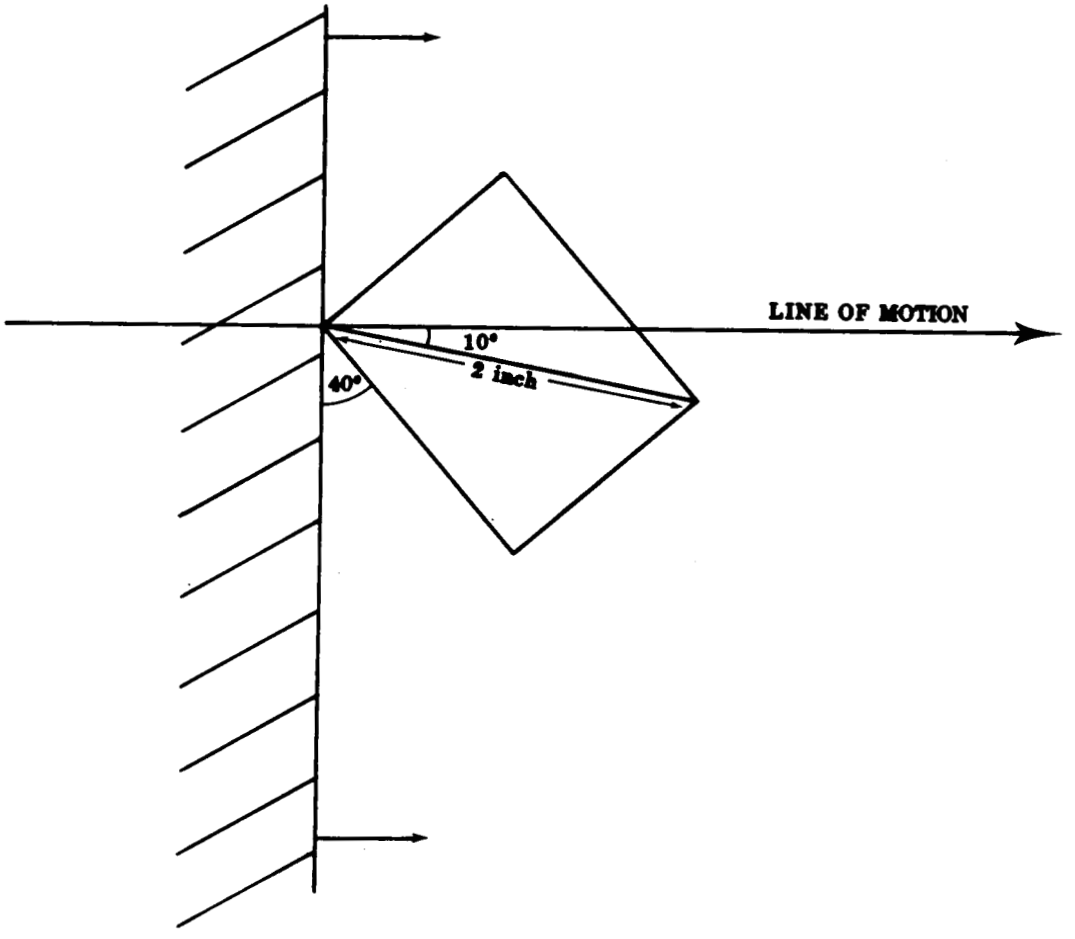

Figure 1-1: The edge of an advancing fence pushing a corner of a sliding object

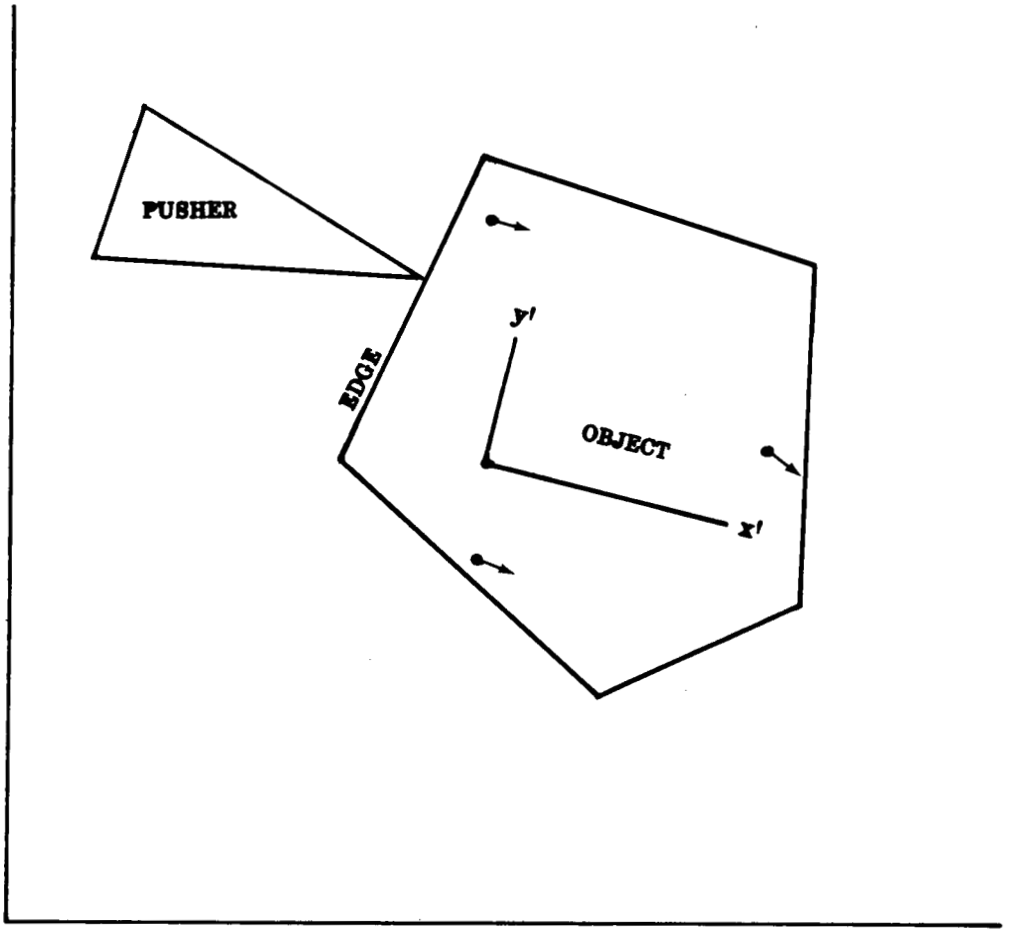

Figure 1-2: A corner of an advancing pusher pushing an edge of a sliding object

table. These support forces may change as the object moves relative to the table. Finding the COR is complicated by the fact that changes in the distribution of support forces under the object substantially affect the motion, i.e., such changes affect the location of the COR. Intuitively, if the support is concentrated near the center of mass (CM), the object will tend to rotate more and translate less than if the support is uniformly distributed over the entire bottom surface of the object.

The distribution of support may be changed dramatically by tiny deviations from flatness in the object's bottom surface (or in the surface it is sliding on.) Any assumption we could make about the form of the support distribution would not be justified in practice. In a previous paper [4] we found the locus of CORs under *all* possible support distributions. It should be possible to read this paper without having read [4], using only the results from the previous paper which are described here in section 2.

Two major simplifications were assumed in the previous work [4]. One was that the coefficient of friction at the pusher-object contact is zero. That assumption is removed in this paper.

The second simplification, common to both papers, is that the object being pushed is a disk with its CM at the center. Given another object of interest (such as a square), we can consider a disk centered at the CM of the square, big enough to enclose it. The radius a of the disk is the maximum distance from the CM of the square to any point of the square. Since any support distribution on the square could also be a support distribution on the disk, the COR locus of the disk must enclose the COR locus of the square. The locus for the disk provides useful bounds on the locus for the real object.

2. Review

The parameters of the COR problem are the point of contact $\vec{c}$ between the pusher and the object, and the angle α between the edge and the line of pushing, as shown in figure 2-1. The values of α and $\vec{c}$ shown are the ones which are useful in considering the motion of the five-sided object shown inscribed in the disk. We do not require the point of contact $\vec{c}$ to be on the perimeter of the disk, as this would eliminate applicability of the results to objects inscribed in the disk. Indeed, for generality we do not even require the point of contact to be within the disk. Similarly, we do not require α to be such that the edge being pushed is perpendicular to vector $\vec{c}$, as it would be if the object were truly a disk. The disk (with radius a), α, $\vec{c}$, and the CM, are shown in figure 2-1. A particularly simple distribution of support forces, in which the support is concentrated at just a "tripod" of points $(\vec{w}_1, \vec{w}_2, \vec{w}_3)$ is indicated, along with what might be the COR for that distribution of support.

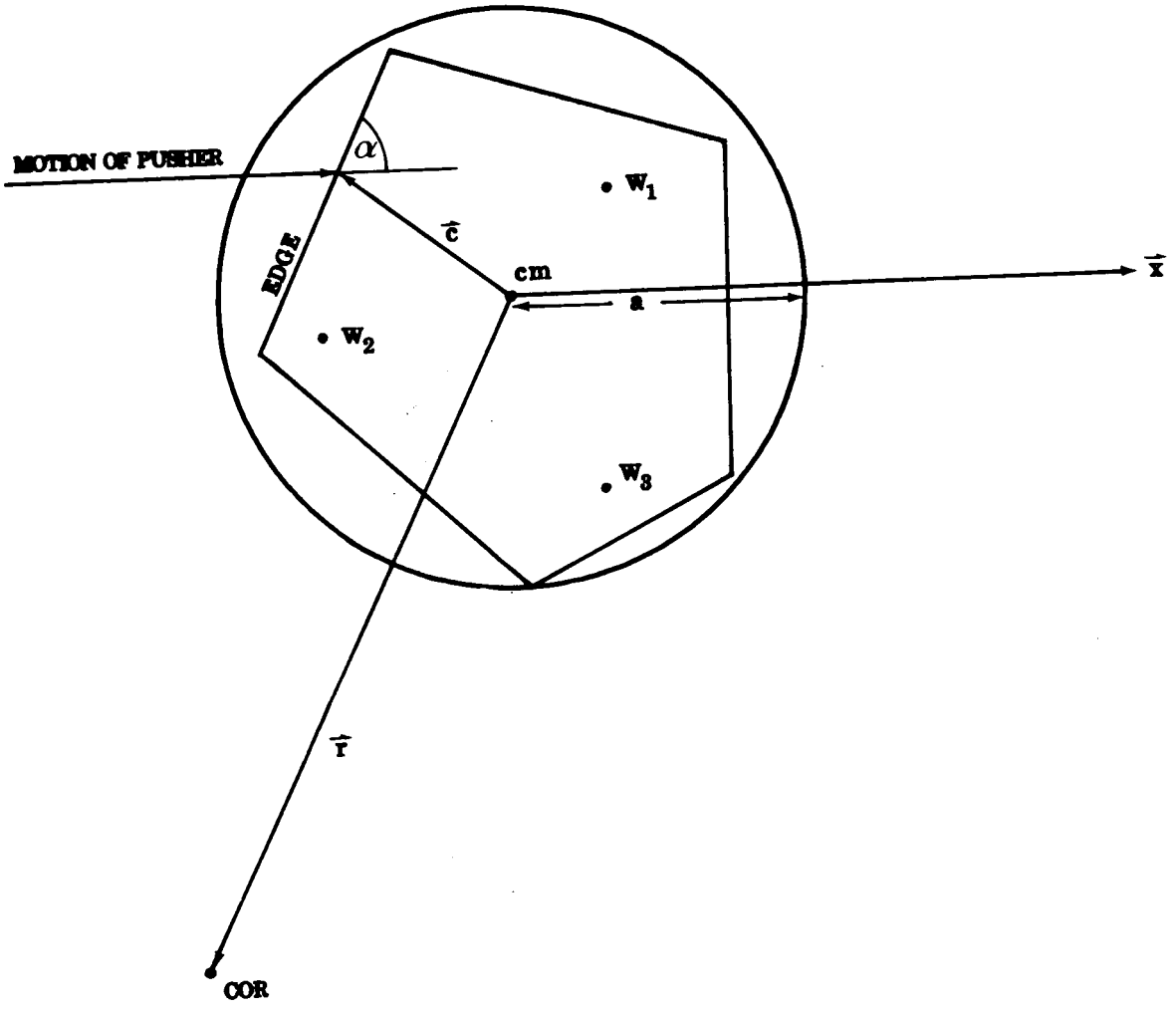

Figure 2-1: Parameters of the pushing problem

Peshkin and Sanderson [4] analyze the motion of the sliding object in detail. The approach is to minimize the energy dissipated by friction with the surface for arbitrary infinitesimal motions. Analytical relations are found between the set of all support distributions, an intermediate formulation called the Q-locus, and the locus of CORs. Boundaries of the COR locus are found by numerical evaluation of the resulting analytical expressions.

Figure 2-2 shows examples of the COR loci found previously [4] for various values of α and $\vec{c}$. In each section the angle α of the edge with respect to the line of pushing is indicated. The edge may be the front edge of a fence pushing a corner of an inscribed object, as in figure 1-1, or it may be an edge of the inscribed object in contact with a pushing point, as in figure 1-2. $\vec{c}$ is the vector from the CM (at the center of the disk) to the point of contact indicated by the arrowhead. The boundary of the COR locus is shown in bold outline. Every point within the locus is the COR for some distribution of support forces on the disk. Results described previously [4] indicate that no distribution of support forces can result in a COR outside the boundary shown.

The COR loci shown were generated under the assumption that the coefficient of friction between the pusher and the object (μ_c) is zero. While the pusher's line of motion is horizontal, the force exerted by the pusher in general will *not* be horizontal. In the special case that $\mu_c = 0$, the force exerted on the object at the point of contact $\vec{c}$ must be perpendicular to the edge. If the angle of that edge (with respect to the x axis) is α, the force must be directed at angle $\alpha - \pi/2$.

When $\mu_c > 0$, the direction of the force exerted on the object by the pusher's horizontal movement cannot in general be determined. It varies, depending on the distribution of support forces beneath the object, which is not known.

The coefficient of friction with the supporting surface (μ_s) does not affect the object's motion if we use a simple model of friction. We assume that μ_s is constant over space, that it is independent of normal force magnitude and tangential force magnitude and direction, and that it is velocity independent. In short, we assume Coulomb friction.

Defining the unit vector $\vec{\alpha} = (\cos\alpha, \sin\alpha)$, we observe that the COR loci have an axis of symmetry about $\vec{\alpha}$. Further, we see in figure 2-2(c), that if the pushing force is directed from the point of contact almost directly through the CM, the maximum distance from the CM to an element of the COR locus becomes great. This distance, called r_{tip}, is infinite if the pushing force is directed at the CM, as shown by Mason [3]. In [4] we found a simple formula for r_{tip}:

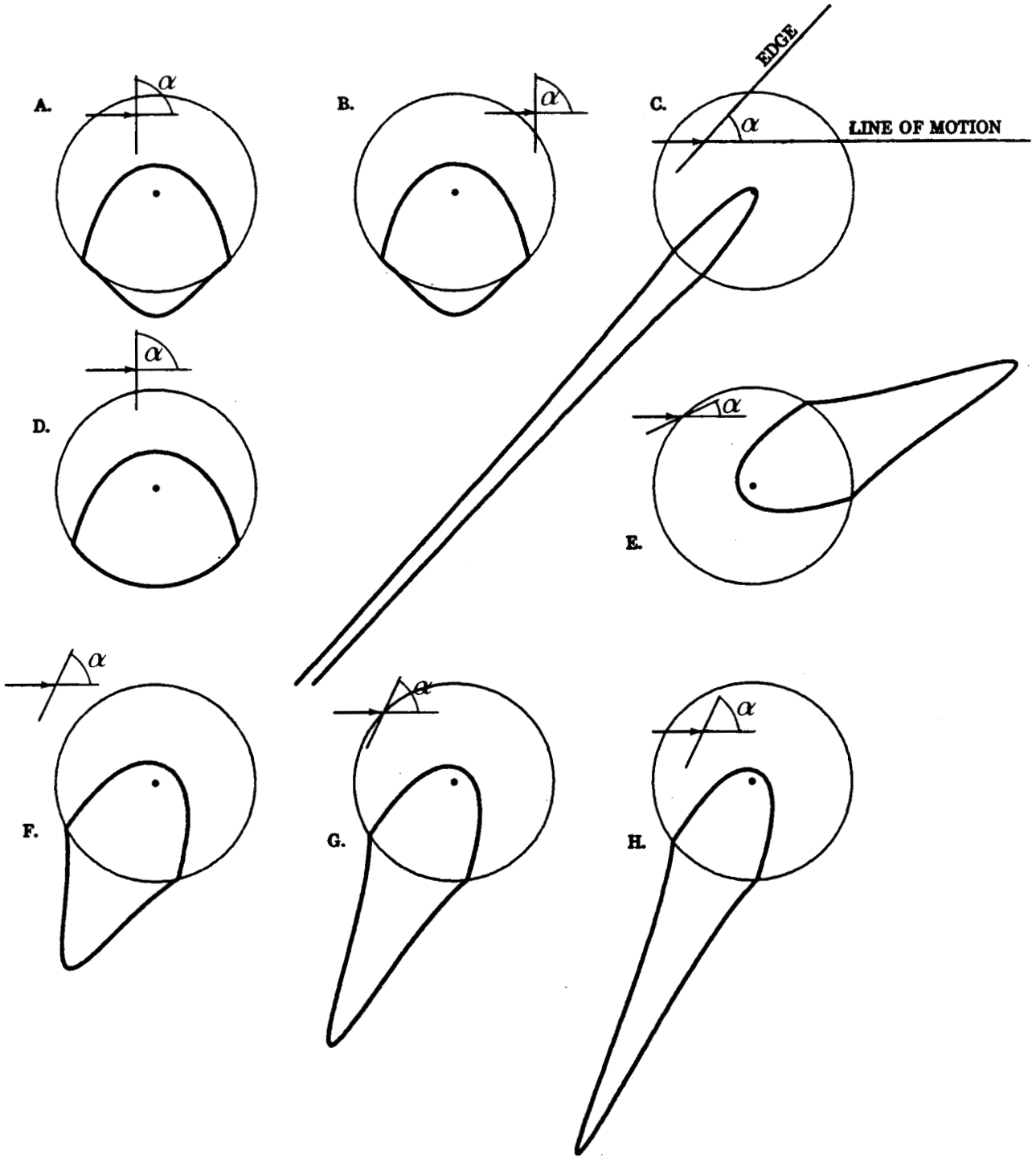

Figure 2-2: Boundaries of the COR locus for various $\vec{c}$ and α

$$r_{tip} = \frac{a^2}{\vec{\alpha}\cdot\vec{c}} \tag{1}$$

As the angle α is varied, the tip of the COR locus traces out a straight line called the *tip line*. The tip line (figure 2-3) is perpendicular to $\vec{c}$, and a distance a^2/c from the CM. It is also possible to find analytically the radius of curvature of the COR locus boundary at the tip:

$$s = \frac{r_{tip}}{\frac{1}{2} + \frac{r_{tip}^4}{a^4}} \tag{2}$$

We will not derive in this paper the equations needed to generate the boundary of the COR locus for a given set of parameters a, α, and $\vec{c}$. (These equations may be found in [4].) It will be assumed that the COR loci can be generated as needed. Here we will show how to *combine* elementary COR loci from the $\mu_c = 0$ case, to find the locus of CORs when $\mu_c > 0$. Many useful results can be found knowing only the qualitative behavior of the COR loci, not the exact forms. The only quantitative information we shall use from previous work [4] is that given by equations 1 and 2, above.

3. The COR Sketch with Contact Friction

3.1. Overview

In our previous work [4], we took $\mu_c = 0$. The pushing force was therefore normal to the edge being pushed. Since the motion of the object can depend only on the force applied to it, we will designate the locus as $\{COR\}_\alpha$ to indicate its dependence on the force angle, which is perpendicular to $\vec{\alpha}$. $\{COR\}_\alpha$ also depends on the point of contact $\vec{c}$ of course.

We know how to generate the COR locus for a given angle of applied force. Unfortunately, when $\mu_c > 0$, it is not possible to tell what the force angle will be. We will describe angular *limits* on the force angle in section 3.2, but within those limits the force angle depends on the distribution of support forces, which is not known. If we already knew that the COR would be at a certain point, however, it would then be possible then to find the force angle.

Our approach to this problem is to seek CORs which are consistent with the force angle which gives rise to them. For each force angle φ within the angular limits, we generate $\{COR\}_\varphi$. For each COR in $\{COR\}_\varphi$ we find the force angle implied. If the force angle implied matches φ, that COR is a possible

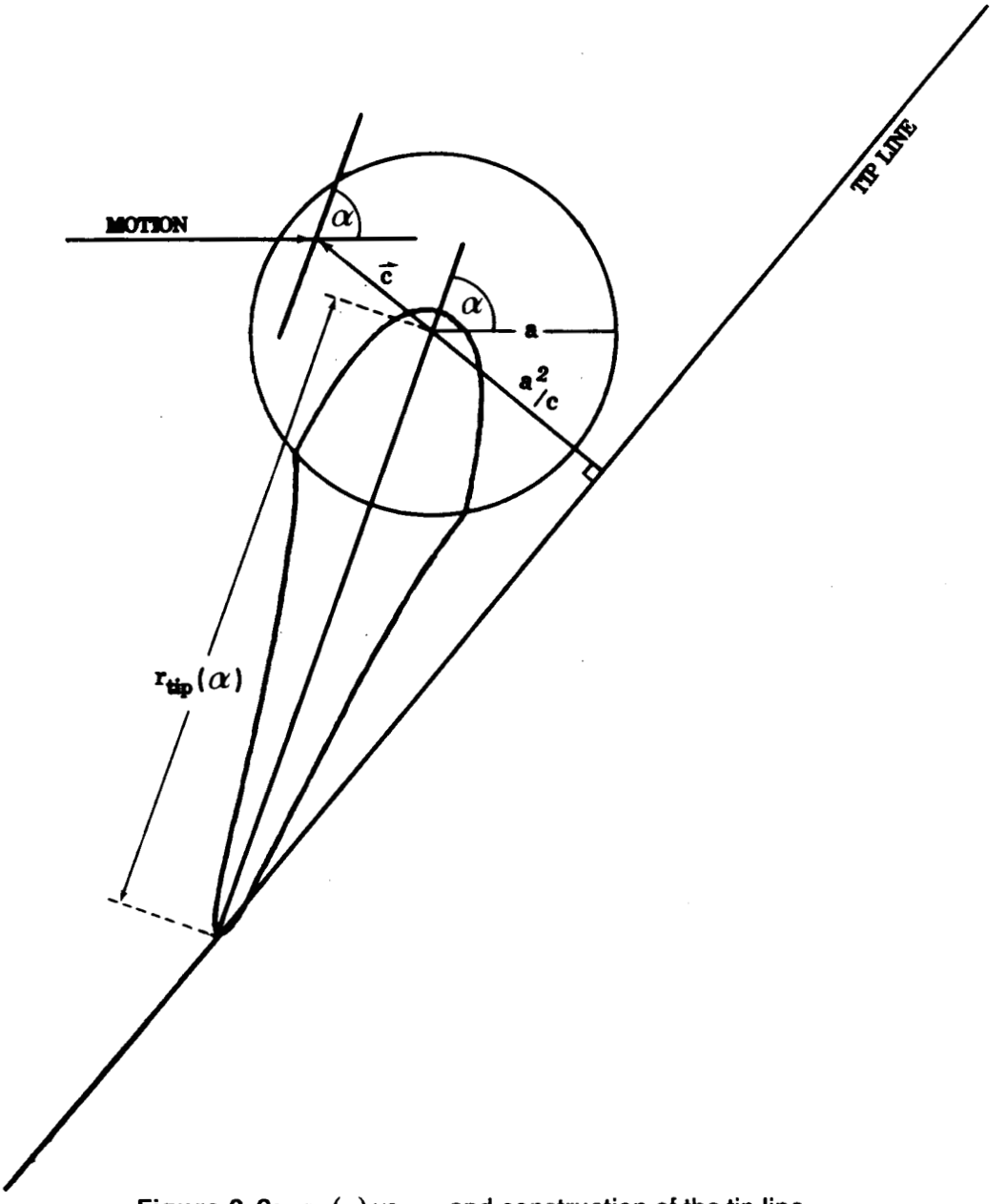

Figure 2-3: $r_{tip}(\alpha)$ vs. α, and construction of the tip line

one for the object. (The above formulation seems to threaten a great deal of computation, which in fact is not required.)

We will refer to the set of consistent CORs as the *COR sketch*, to distinguish it from the elementary COR loci $\{COR\}_\varphi$ produced for known force angles. Several elementary COR loci will be used in the construction of the COR sketch. In the figures, these COR loci will be left visible in outline, while the actual COR sketch —— the consistent CORs —— will be shown shaded.

3.2. Contact Friction and the Friction Cone

Let μ_c be the coefficient of friction between the pusher and the object. If $\mu_c > 0$, two distinct modes of behavior of the system are possible: *sticking* and *slipping*. In figure 1-1, sticking means that the element of the fence in contact with the object remains invariant as the pusher's motion proceeds. In figure 1-2, sticking means the element of the object which is in contact with the pusher remains invariant as the pusher's motion proceeds. Slipping is simply the case in which either the element of the pusher or the element of the object, which are in contact with each other, changes as the motion proceeds.

Define

$$\nu = \tan^{-1}\mu_c \tag{3}$$

In figure 3-1 we construct a *friction cone*, of half angle ν, at the point of contact $\vec{c}$. The cone is centered on the edge normal, at angle $\alpha - \pi/2$ relative to horizontal. Note that the edge may be either that of a fence, where it contacts a corner of the object (as in figure 1-1), or an edge of the object, where it is touched by a corner of the pusher (as in figure 1-2).

The component of the applied pushing force tangential to the edge, $F_{\|}$, is due to μ_c. Its magnitude cannot exceed $\mu_c F_{\perp}$, where $F_{\perp}$ is the component of force normal to the edge. Therefore the total applied force vector must lie within the friction cone.

If we attempt to apply a force to the edge at an angle outside of the friction cone, friction cannot support the tangential component. The result is slipping along the edge, and the actual applied force is directed along one extreme of the friction cone. If we apply a force within the friction cone, friction is sufficient to support the tangential component of force, and slipping will not occur: we have sticking.

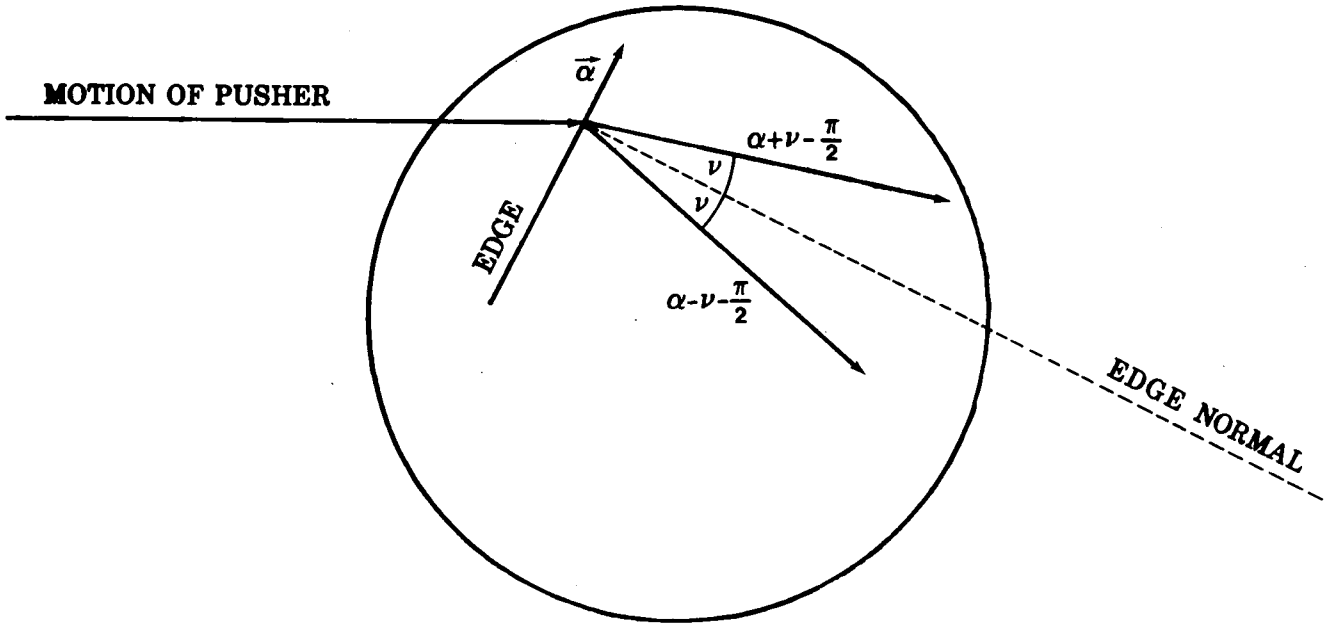

Figure 3-1: Construction of the friction cone

In short, slipping is only consistent with a force vector at one extreme of the friction cone, while sticking is only consistent with a force vector within the friction cone. It is not usually possible to tell if slipping or sticking will occur: often, depending on the distribution of support forces, either may occur.

3.3. Sticking and Slipping Zones

In this section we presume that the COR is known: a single point is the COR for the object. We divide the plane into three zones, called the *sticking line*, the *up-slipping zone* and the *down-slipping zone*. (Figure 3-2). The up-slipping and down-slipping zones are regions of the plane with positive areas, while the sticking line is merely a line, but all three will be collectively designated "sticking and slipping zones." The motion of the object is qualitatively different for the COR falling in each of the three zones.

The sticking line is the line perpendicular to the pusher's line of motion, intersecting the point of contact between pusher and object, (i.e. $\vec{c}$ lies on the sticking line). Since we choose to draw the pusher's line of motion horizontally, the sticking line is vertical. The sticking line divides the down-slipping zone, on its left, from the up-slipping zone, on its right. Also shown in figure 3-2 is the edge normal line. Above this line, the up-slipping and down-slipping designations are reversed. The area above the edge normal will be unimportant, however.

3.3.1. Sticking Line

First consider the object's motion when the COR is on the sticking line. Recall that the motion of any point of the object is perpendicular to the vector from the COR to that point. If the COR lies on the sticking line, the object's motion at the point of contact is perpendicular to the sticking line, and is therefore parallel to the pusher's line of motion.

Since the pusher's line of motion and the object's motion at the point of contact are parallel, the pusher and the object, at the point of contact, travel along together. There is no need for one to slip relative to the other; the object and the pusher are *sticking* at the point of contact.

3.3.2. Slipping Zones

Now suppose that the COR is in the down-slipping zone. The object's motion at the point of contact has a downward component, relative to the pusher's line of motion. The pusher-object contact must be *slipping*, with the object moving down relative to the pusher.

Similarly, if the COR is in the up-slipping zone, the object at the point of contact moves up relative to the pusher as the pusher advances.

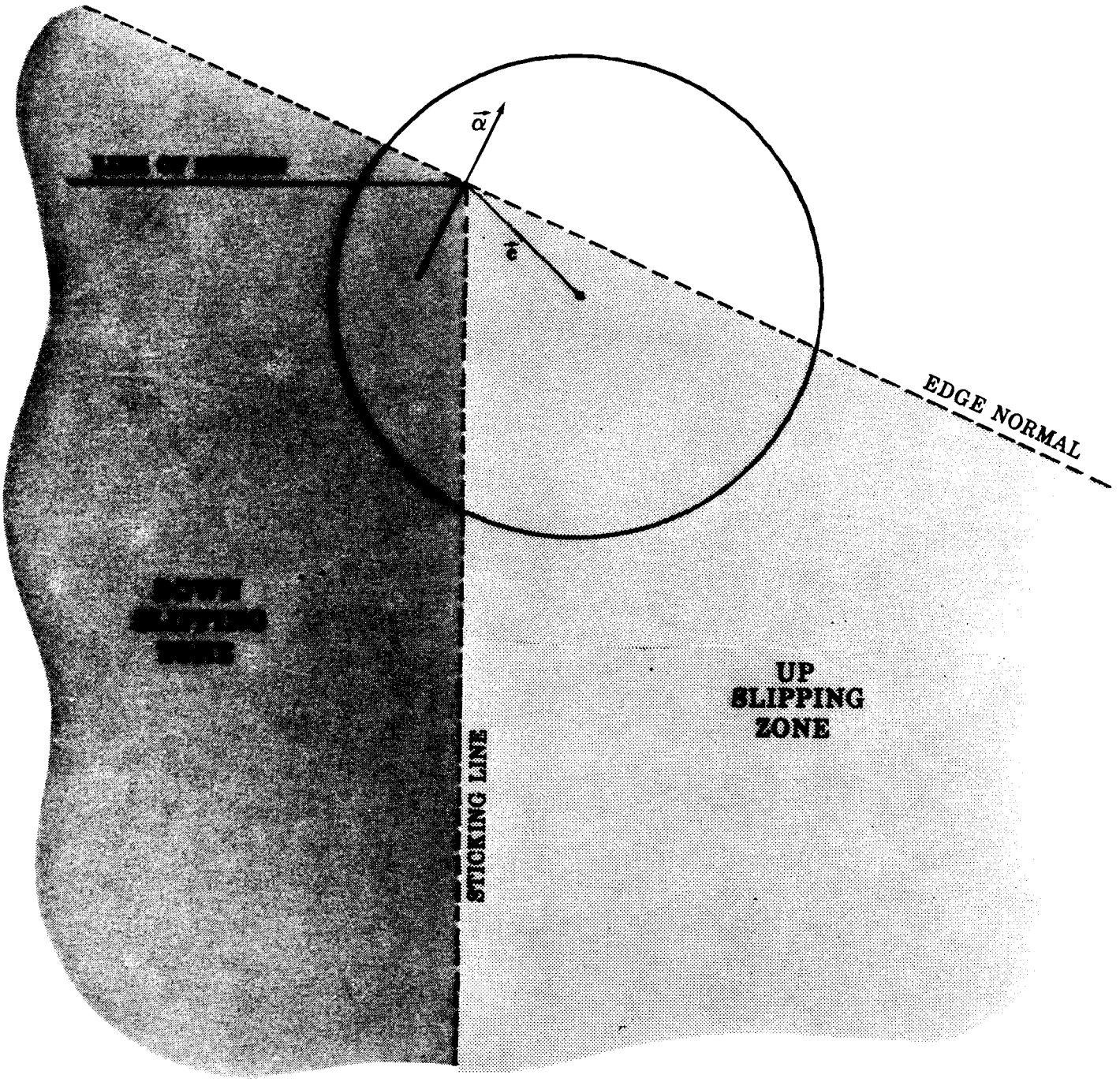

Figure 3-2: Construction of zones: up-slipping, down-slipping, and sticking line

3.4. Consistency for Slipping

If we know that the object is slipping relative to the pusher (and whether up or down), then the force angle is known: it is at one extreme of the friction cone, perpendicular to $\alpha \pm \nu$.

If the COR lies in the down-slipping zone, the object moves *down* as the pusher advances. Therefore the force angle must be along the upper extreme of the friction cone, at angle $\alpha + \nu - \pi/2$. Similarly, if the COR lies in the up-slipping zone, the object moves *up* as the pusher advances, and the force angle must be along the lower extreme of the friction cone, at angle $\alpha - \nu - \pi/2$.

Combining the above observations, we see that if slipping occurs, the COR must be either in $\{COR\}_{\alpha+\nu}$ and the down-slipping zone, or in $\{COR\}_{\alpha-\nu}$ and the up-slipping zone. These two intersection regions are called the *down-slipping locus* and the *up-slipping locus*.

The down-slipping and up-slipping loci are two components of the COR sketch, because every COR in either locus is consistent with the force angle that was used to generate it. We construct the down-slipping locus of the COR sketch by intersecting the down-slipping zone (left of the sticking line) with $\{COR\}_{\alpha+\nu}$. We construct the up-slipping locus of the COR sketch by intersecting the up-slipping zone (right of the sticking line) with $\{COR\}_{\alpha-\nu}$.

In figure 3-3, $\{COR\}_{\alpha+\nu}$ and $\{COR\}_{\alpha-\nu}$ are shown in outline. The down-slipping and up-slipping loci are the shaded areas left and right of the sticking line respectively.

3.5. The Sticking Locus

The third set of consistent CORs belong to the *sticking locus*. The sticking locus, together with the up-slipping and down-slipping loci whose construction was described above, are all the CORs consistent with the force angle they presume. The three consistent loci constitute the COR sketch.

If the COR lies on the sticking line, sticking occurs. The force angle can be anywhere in the friction cone, i.e., between $\alpha - \nu - \pi/2$ and $\alpha + \nu - \pi/2$. The sticking locus is therefore the intersection of the sticking line with the union, over all φ perpendicular to a force angle within the friction cone, of $\{COR\}_{\varphi}$. The sticking locus is shown as a bold section of the sticking line in figure 3-3.

As discussed above, the two slipping loci are $\{COR\}_{\alpha\pm\nu}$, possibly cut off by the sticking line. In calculating either slipping locus, the force angle is known: it is $\alpha \pm \nu - \pi/2$. But in calculating the sticking locus, (which is just a simple line segment), the force angle is not known, except that it lies within the friction cone. To find the endpoints of the sticking locus exactly, we could form every locus

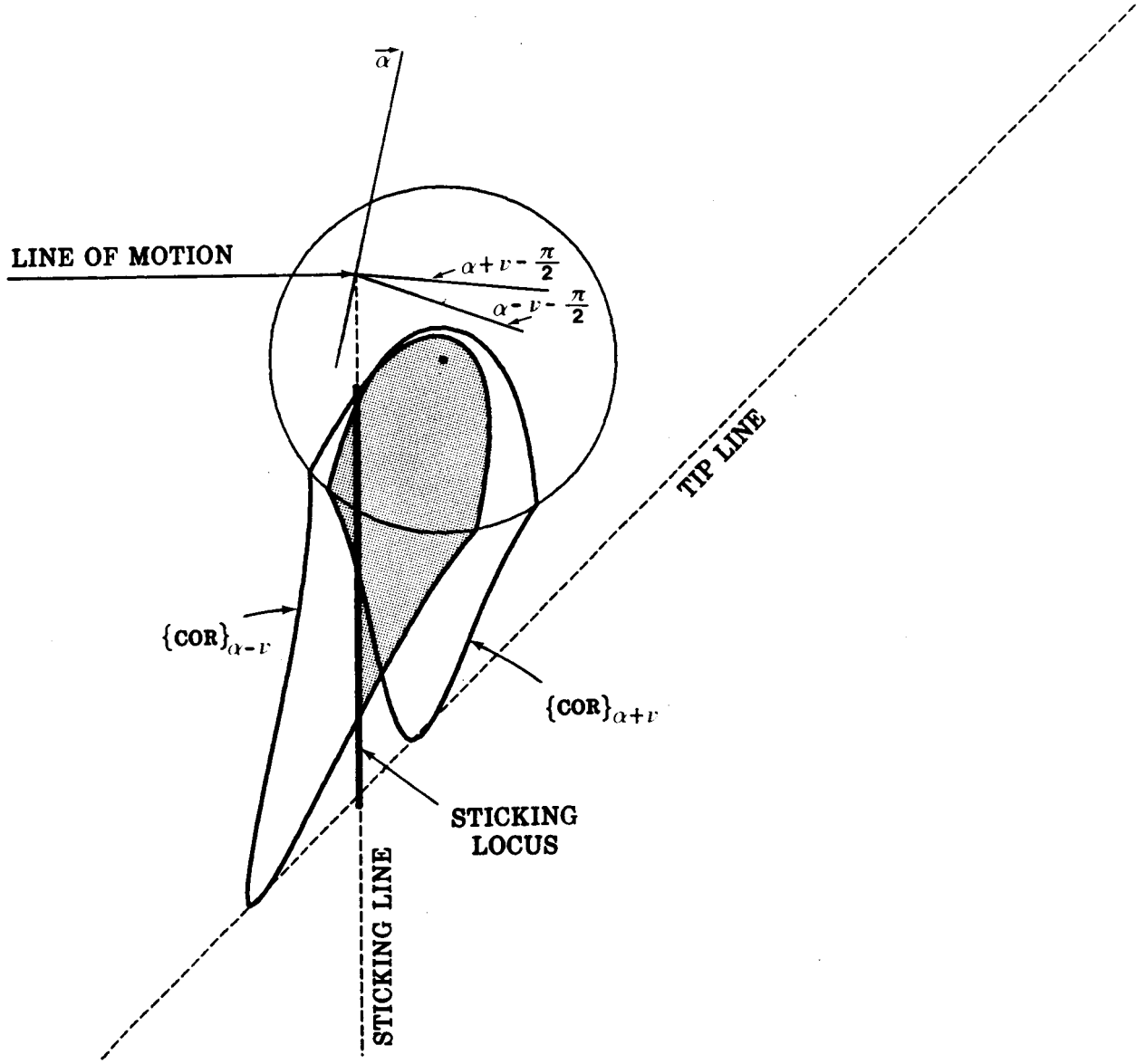

Figure 3-3: Construction of the COR sketch

$\{COR\}_\varphi$, for $\alpha-\nu<\varphi<\alpha+\nu$, and intersect each locus with the sticking line. The union of these intersections is the sticking locus. This is not an efficient method.

The lower endpoint of the sticking locus is of particular interest. It is possible to approximate it, and to bound the error of our approximation, by using the tip-line construction described in section 2, equation 1 and shown in figure 2-3. The procedure for finding the sticking locus described above is to form every locus $\{COR\}_\varphi$, for $\alpha-\nu<\varphi<\alpha+\nu$, and intersect each locus with the sticking line. As we vary φ, $\{COR\}_\varphi$ varies continuously from $\{COR\}_{\alpha-\nu}$, which is outlined in figure 3-3, to $\{COR\}_{\alpha+\nu}$, also shown outlined. The tip of the extreme loci, as well as of all intermediate loci, fall on the tip line. The tip line is shown dotted in figure 3-3.

Were it not for the fact that each $\{COR\}_\varphi$ locus drawn dips slightly below the tip line, the lower endpoint of the sticking locus would be exactly at the tip line. We will use this approximation. The small error so introduced will be dealt with in section 4.1.

Using the tip line to approximate the lower endpoint of the sticking locus in this way depends on an unstated assumption: that the tip of $\{COR\}_{\alpha-\nu}$ lies to the left of the sticking line while the tip of $\{COR\}_{\alpha+\nu}$ lies to the right of the sticking line. This assumption is necessary so that the tip of some intermediate locus $\{COR\}_\varphi$ will intersect the sticking line. In section 3.7 we will deal methodically with this problem.

The shaded slipping loci and the bold sticking locus of figure 3-3 contain all the possible locations of the COR.

3.6. Possible Configurations of an Elementary COR Locus

The down-slipping, up-slipping , and sticking *loci* play an important part in the rest of this work. It is worth describing the qualitatively different ways in which an elementary COR locus $\{COR\}_\alpha$ can intersect the three *zones* (down-slipping, up-slipping, and sticking line) in order to form the loci. These qualitatively different types of intersections will be called distinct *elementary configurations*. Later we will describe the qualitatively different COR sketches which can occur; the latter will be called distinct *sketches*. Two COR loci are used in the construction of a COR sketch, so there are more distinct sketches than distinct elementary configurations.

For a given contact point $\vec{c}$, changing α yields four distinct elementary configurations of the resulting COR loci. In figure 3-4(A), the *pure slipping* elementary configuration, the entire COR locus falls in the up-slipping zone. In figure 3-4(B), the COR intersects all three zones, but the tip of the locus falls

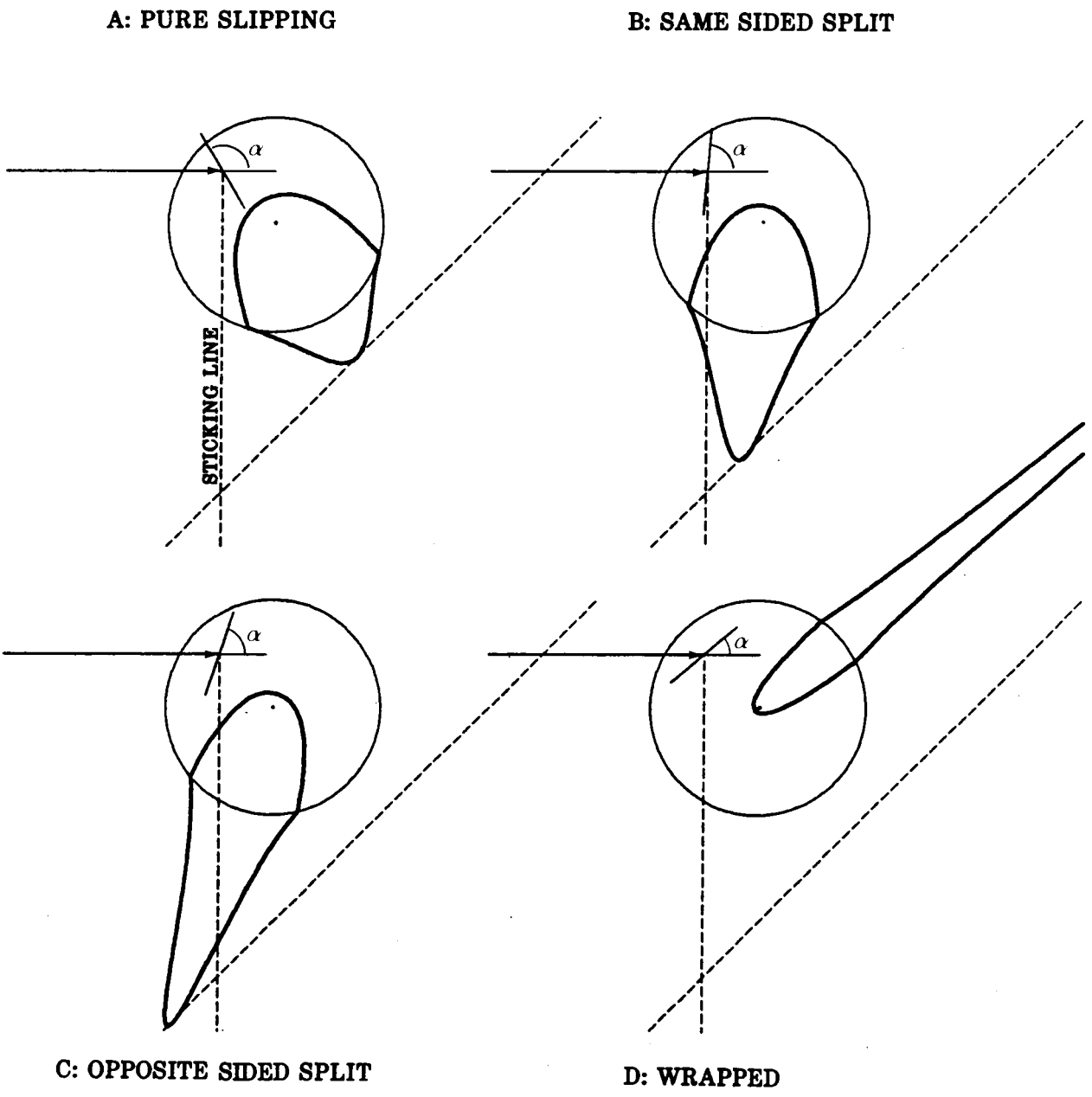

Figure 3-4: Possible elementary configurations of the COR locus with respect to the sticking line

on the same side of the sticking line as the CM. This is the *same-sided-split* elementary configuration. As α is further decreased, the tip of the COR locus crosses the sticking line, entering the *opposite-sided-split* elementary configuration, as shown in figure 3-4(C). Finally, when α decreases to the point where the edge normal at $\vec{c}$ intersects the CM, the COR locus goes to infinity [3]. The COR at infinity implies pure translation (with no rotation) of the object as the pusher advances. Beyond this point the object's sense of rotation switches from clockwise to counterclockwise. For our purposes in constructing a COR sketch, counterclockwise rotation is unphysical [3], and so we will class this, and pure translation as one elementary configuration, the *wrapped* elementary configuration, as shown in figure 3-4(D). No part of a "wrapped" locus will ever contribute to the COR sketch, yet we will continue to draw its outline as shown in the figure.

The same four elementary configurations can be defined (now with increasing α) when the sticking line is to the right of the CM (Figure 3-5).

3.7. Possible Distinct COR Sketches

Depending on α and μ_c, each of the two elementary COR loci $\{COR\}_{\alpha\pm\nu}$ used in constructing the COR sketch may be any of the four elementary configurations described in section 3.6 (pure slipping, same-sided split, opposite-sided split, or wrapped). There are nine possible distinct sketches composed of two elementary configurations, as shown in figure 3-6. (Of the 4^2 combinations, 6 are eliminated because the tip of $\{COR\}_{\alpha+\nu}$ cannot be left of the tip of $\{COR\}_{\alpha-\nu}$. The one sketch in which both $\{COR\}_{\alpha\pm\nu}$ are "wrapped" elementary configurations is inconsistent with clockwise rotation of the object.)

It is worth looking carefully at each sketch, in particular to understand the construction of the sticking locus. The sticking locus is the intersection of $\{COR\}_{\varphi}$ with the sticking line, as φ is swept from $\alpha+\nu$ to $\alpha-\nu$. The sweeping is always *clockwise*. In sketch (G), sweeping clockwise means sweeping from the pure slipping locus, clockwise, to the wrapped locus. The intermediate loci therefore do intersect the sticking line, even though neither locus $\{COR\}_{\alpha\pm\nu}$ does. Unless this is understood the origin of the sticking locus in sketches (G) and (H) will remain mysterious.

Several of the sketches shown in figure 3-6 have interesting properties. In sketch (A), the object must slip up relative to the pusher. In sketches (B) and (D), the object must stick or slip up. In sketch (G), the object must stick to the pusher. In sketches (H) and (I), the object must stick or slip down. In the remaining sketches (C), (E), and (F), either mode of slipping, or sticking, is possible, depending on the distribution of support.

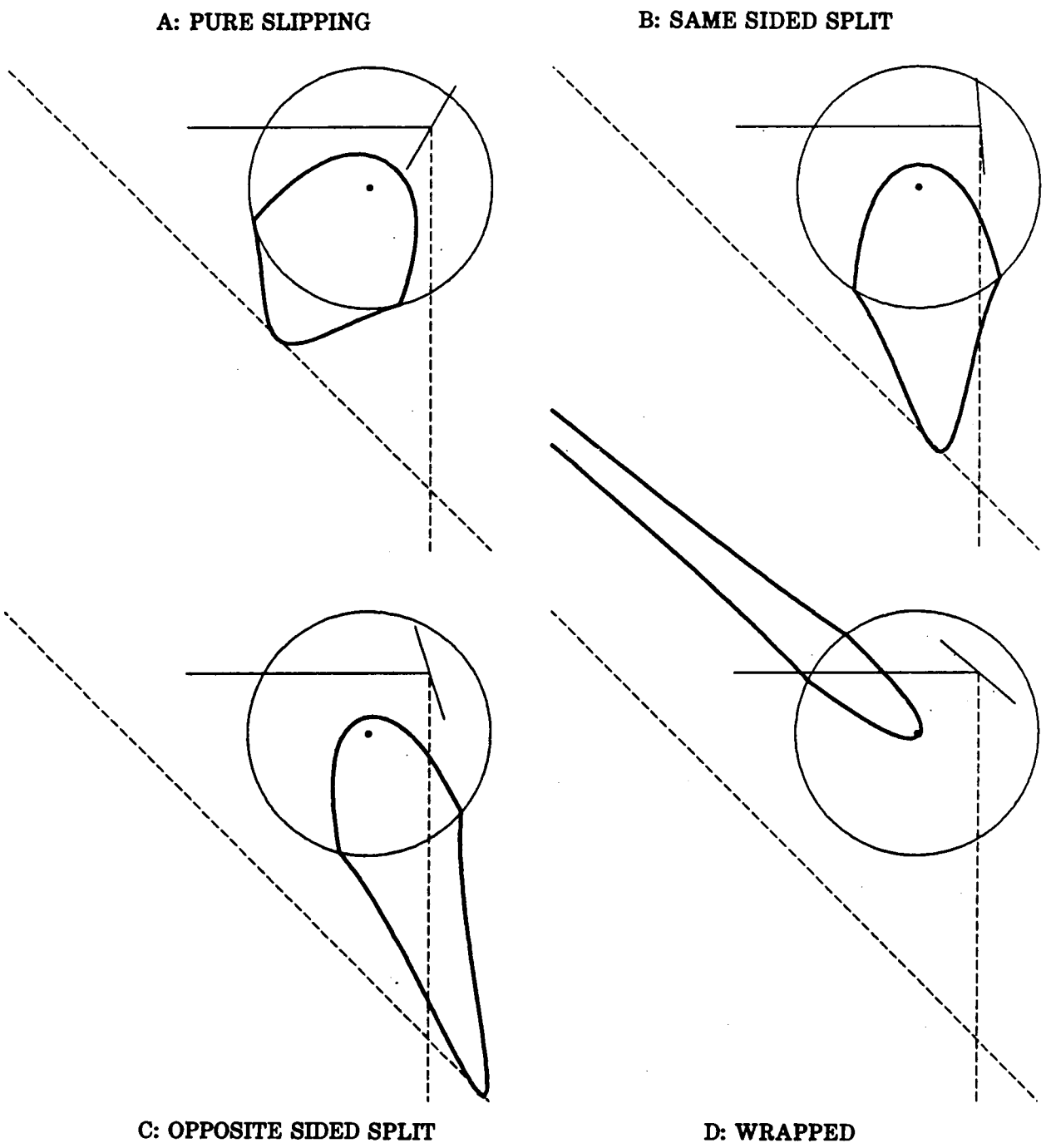

Figure 3-5: Possible elementary configurations, when the sticking line is to the right of the CM

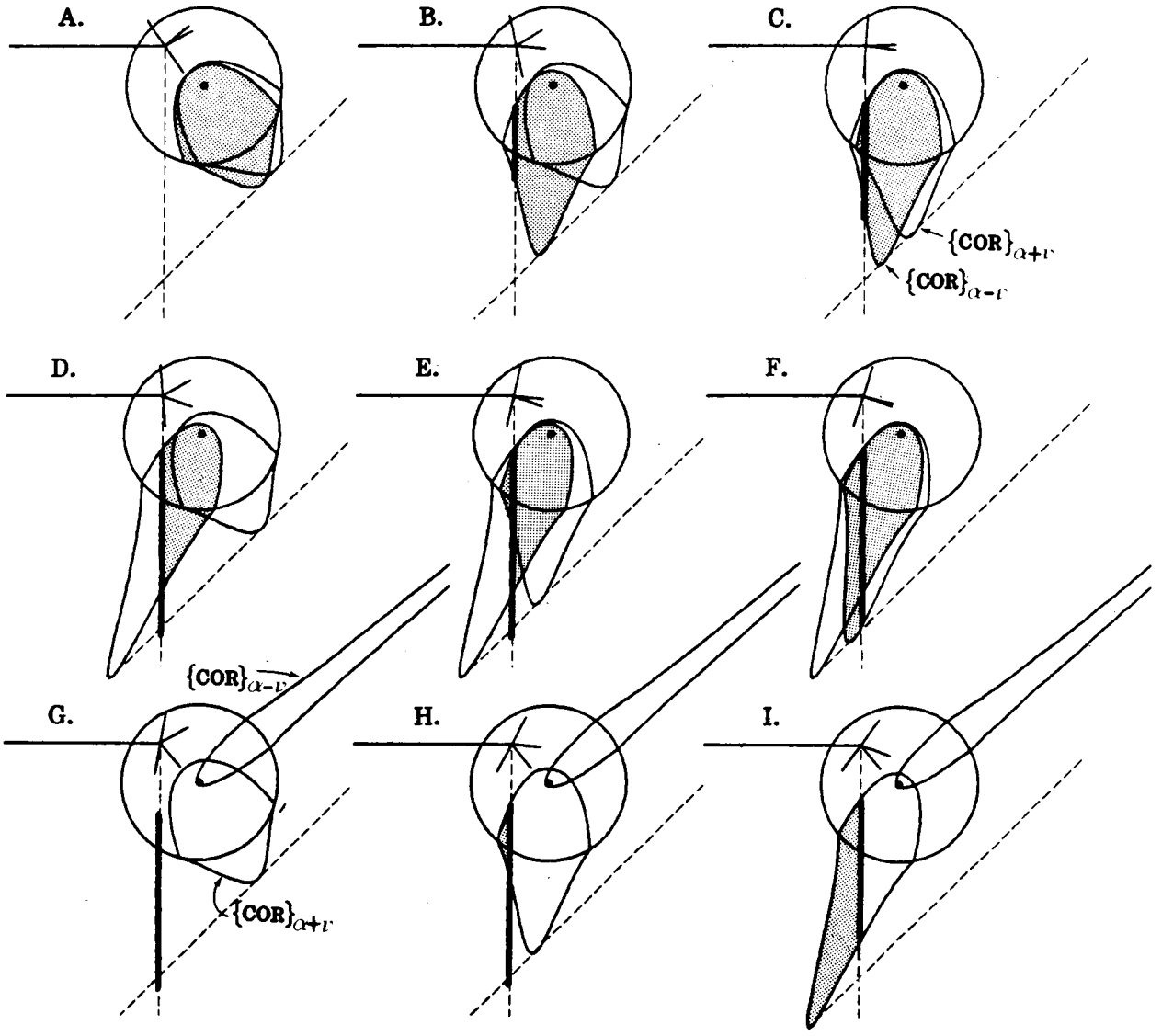

Figure 3-6: Nine distinct COR sketches with respect to the sticking line

Analogous qualitative results are possible when the point of contact $\vec{c}$ is to the right of the CM. The distinct COR sketches for this case can be obtained from those shown in figure 3-6 by reflecting about a vertical axis. (The pusher's motion should still be considered left-to-right, however.) The distinct sketches for counterclockwise rotation of the object may be obtained by reflecting about a horizontal axis.

3.8. Summary: Instantaneous Motion

We have shown how to find all possible instantaneous motions of a pushed sliding object, given only the parameters α, $\vec{c}$, and a. In some cases it is possible to say with certainty that a particular kind of motion, such as sticking, can or cannot occur. The set of possible CORs, as found by constructing the COR sketch, describes completely the possible instantaneous motions of the object as long as those parameters remain in effect. Usually however, the instantaneous motion which results changes the parameters (except the radius a), so that a new COR sketch must be constructed.

3.9. Strategy for Gross Motion

Often we wish to calculate not the bounds on the instantaneous direction of motion, as above, but bounds on a gross motion of the object which can occur concurrently with some other gross motion of known magnitude. (For instance, we may wish to find bounds on the displacement of the pusher which occurs while the object rotates 15 degrees.) Our approach to dealing with gross motion follows a definite strategy, which will be illustrated in the sample problems solved in sections 4, 5, and 6.

Suppose we wish to find the greatest possible change in a quantity x, while quantity β changes from $\beta_{initial}$ to β_{final}. From the geometry of the problem we find a *differential equation of motion* relating the instantaneous motions dx and $d\beta$. We then construct the COR sketch for each value of β. In each sketch we locate the possible COR which maximizes $dx/d\beta$. Using that COR, we integrate the differential equation of motion from $\beta_{initial}$ to β_{final}, yielding an upper bound for the quantity x.

Sometimes the possible COR which maximizes $dx/d\beta$ can be found analytically, or at least approximated analytically, and sometimes it must be found numerically. When an analytical solution is found, it may or may not be possible to integrate the differential equation of motion in closed form using that analytical solution. The examples which follow illustrate all of these situations.

4. Example: Aligning an Object by Pushing with a Fence

In this example, we wish to find the maximum distance a fence must advance after first contacting an object, in order to assure that an edge of the pushed object has rotated into contact with the fence. A typical initial configuration is shown in figure 4-1, with the object shown shaded. (Note that the fence does not advance perpendicular to its front edge.) The final configuration is shown in figure 4-2.

Also shown in figure 4-1 is the COR sketch for the initial configuration, and the angle β between the line of motion and the line from the point of contact to the CM. β is also the angle between the tip line and the sticking line. Angle β changes from 45 degrees initially in figure 4-1 to 80 degrees in the final configuration, figure 4-2. Note that a one degree rotation of the object about the COR will produce a one degree change in β as well. We wish to find the advance x of the pusher (fence) required to change β by 35 degrees.

The object's rate of rotation about the COR $d\beta$, for advance of the pusher dx, is given by

$$dx = y\, d\beta \tag{4}$$

where y is the distance from the line of motion to the COR. To find the maximum required pushing distance, we must find the maximum value of y for any possible COR.

Reviewing the nine distinct COR sketches in figure 3-6, we see that the COR responsible for the greatest y, i.e., the COR farthest from the line of motion, is the COR at the lower endpoint of the sticking locus in sketches (D), (E), (G), and (H). In sketches (A), (B), (C), (F), and (I), it is the COR at the bottom of one of the loci $\{COR\}_{\alpha\pm\nu}$ which is farthest from the line of motion. If the tips of the two loci $\{COR\}_{\alpha\pm\nu}$ fall on the same side of the sticking line, the lowest COR is an element of one of the two loci $\{COR\}_{\alpha\pm\nu}$. We will call this behavior *slipping-lowest*. If the tips of the two loci $\{COR\}_{\alpha\pm\nu}$ fall on opposite sides of the sticking zone , the lowest COR is the lowest point of the sticking locus. We will call this behavior *sticking-lowest*. (For the purposes of the rule given here, the "wrapped" loci in sketches (G), (H), and (I) count as having their tip to the left of the sticking line.)

It is possible to have a transition from slipping-lowest behavior to sticking-lowest behavior within a pushing operation, as β increases. Such a transition occurs when the tip of one of the loci $\{COR\}_{\alpha\pm\nu}$ passes through the sticking line. In figure 4-3, for example, it is $\{COR\}_{\alpha+\nu}$ which passes through the sticking line. In figure 4-4, the tip of the COR locus intersects the sticking line. We may derive the condition for intersection:

$$a^2 + c^2 = -a^2 \tan\beta\, \tan(\alpha\pm\nu+\beta) \tag{5}$$

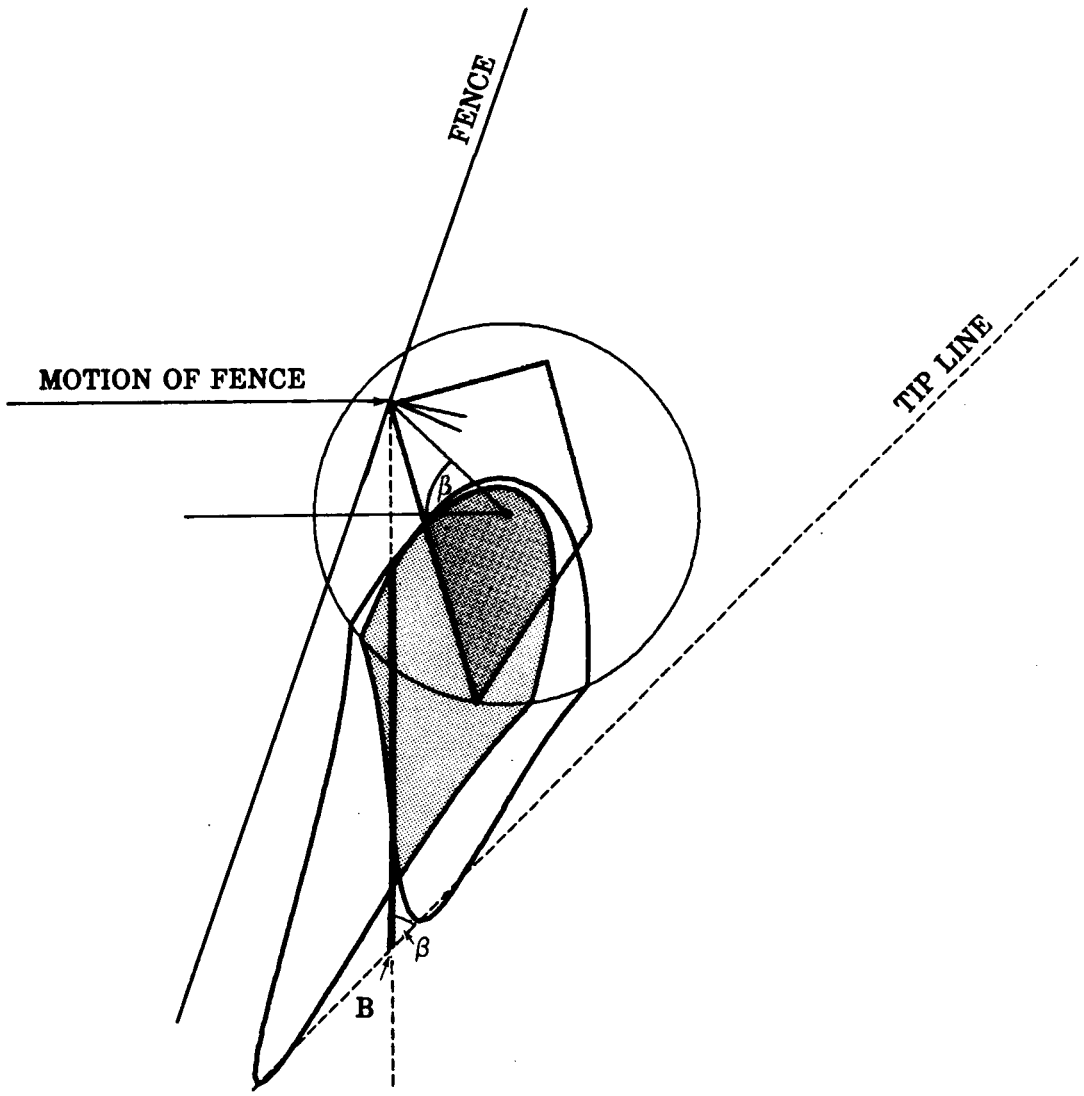

Figure 4-1: Initial orientation of the fence and pushed object

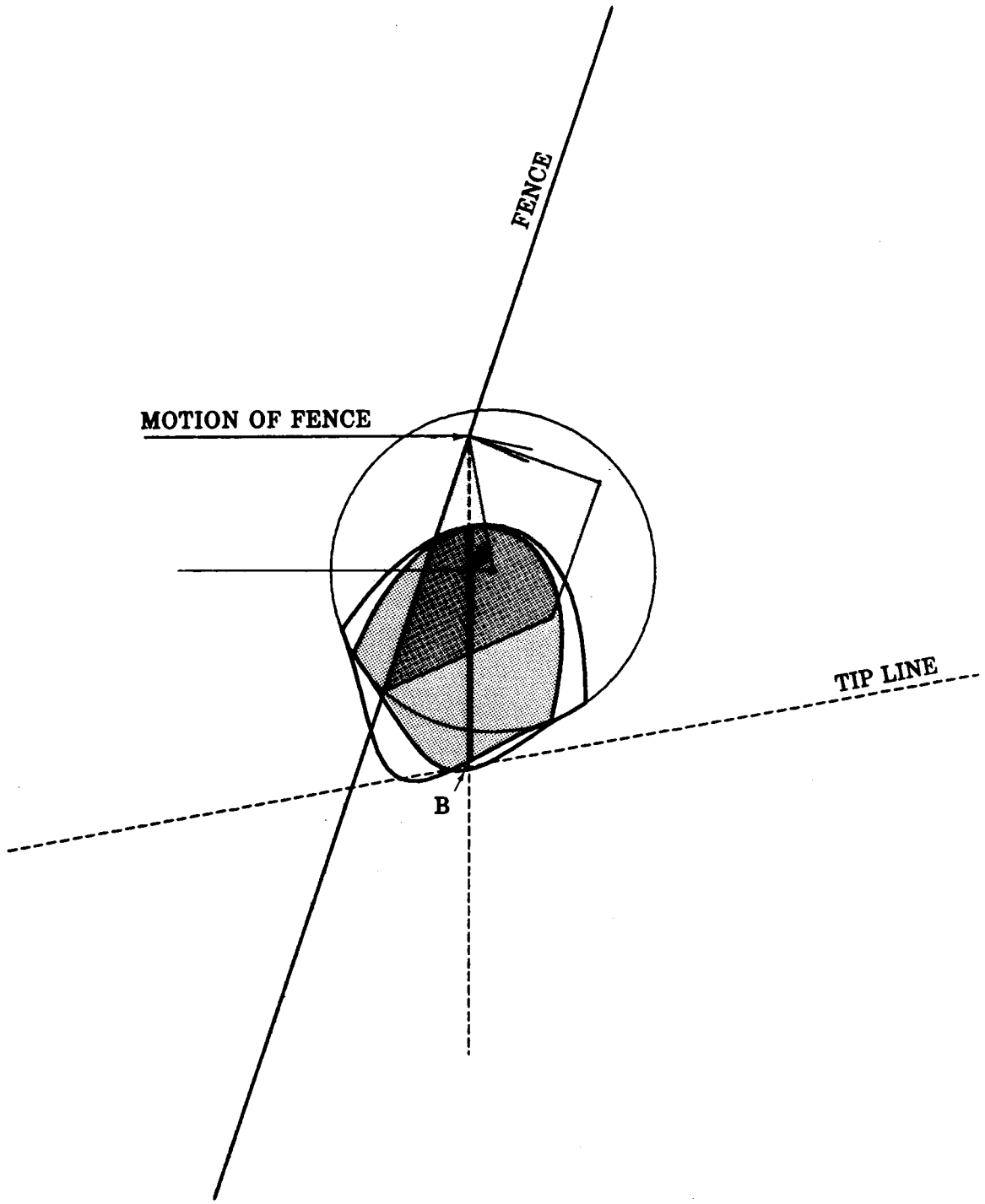

Figure 4-2: Final (aligned) orientation of the fence and pushed object

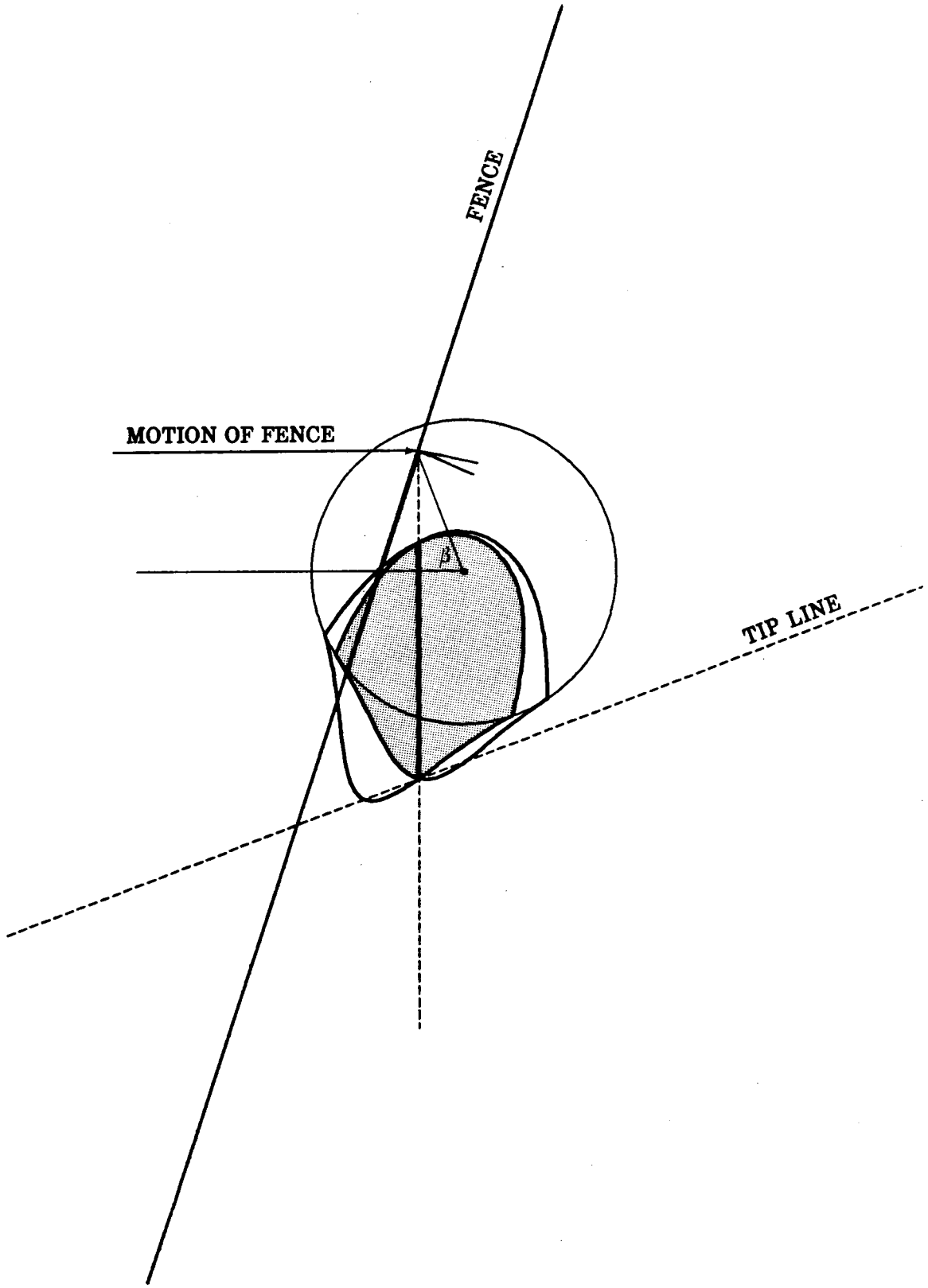

Figure 4-3: Transition from sticking-lowest to slipping-lowest behavior

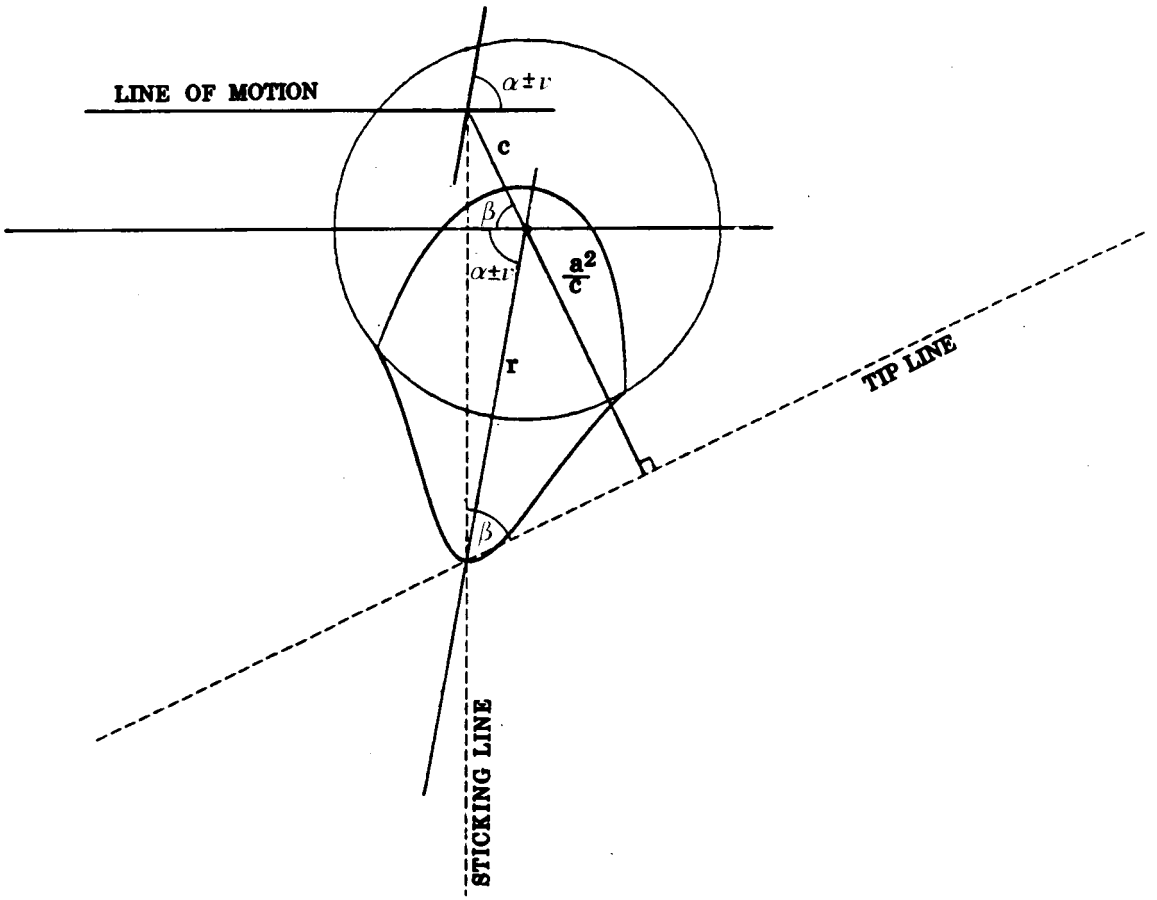

Figure 4-4: Geometric construction for equations 5 and 6

The tip of locus $\{COR\}_{\alpha\pm\nu}$ is on the same side of the sticking line as the CM when the left side of equation 5 is less than the the right side. The value of β at which the tip crosses the sticking line may be found by solving equation 5 for β:

$$\tan\beta_{transition} = \frac{c^2\tan(\alpha\pm\nu) \pm (c^4\tan^2(\alpha\pm\nu) - 4a^2(a^2+c^2))^{1/2}}{2a^2} \tag{6}$$

The pushing distances required to advance β from its initial value to the transition, and from the transition to the final value, must be evaluated separately. In our example, the locus $\{COR\}_{\alpha+\nu}$ is type same-sided split initially, but changes to type opposite-sided split. Using equation 6 we find $\beta_{transition} = 69.4$ degrees, as shown in figure 4-3.

4.1. Approximating the Lowest COR by an Element of the Tip Line

In either behavior regime, sticking-lowest or slipping-lowest, the lowest COR is only slightly below the tip line. If the radius of curvature of the tip of the COR locus were zero, the lowest COR would fall on the tip line. Here we will neglect the finite curvature of the tip, and approximate the lowest point of a COR locus (or of the sticking locus) by some element of the tip line. In section 4.2 we will bound the error this approximation produces.

4.1.1. Slipping-Lowest Behavior

In figure 4-2 the lowest COR is an element of $\{COR\}_{\alpha+\nu}$, labeled "B". Here we find the distance from the line of motion to the most distant COR, when that COR is an element of $\{COR\}_{\alpha\pm\nu}$. Using figure 4-5 the distance can be approximated as

$$y_{slip\,low} = c\sin\beta + r_{tip}\sin(\alpha\pm\nu) \tag{7}$$

$$\text{where } r_{tip} = \frac{-a^2}{c\cos(\alpha\pm\nu+\beta)}.$$

from equation 1. To find the maximum required pushing distance it is only necessary to integrate $dx = y\,d\beta$ with y as given here. We obtain the indefinite integral

$$x = -c\cos\beta - \frac{a^2\sin(\alpha\pm\nu)}{2c}\log\left|\frac{1+\sin(\alpha\pm\nu+\beta)}{1-\sin(\alpha\pm\nu+\beta)}\right|. \tag{8}$$

Since, in the example being considered, the motion from $\beta_{transition} = 69.4$ degrees until $\beta_{final} = 80$ degrees falls in the slipping-lowest behavior regime, we simply evaluate x at these two angles and subtract. The distance Δx obtained is one component of the maximum required pushing distance to align the object.

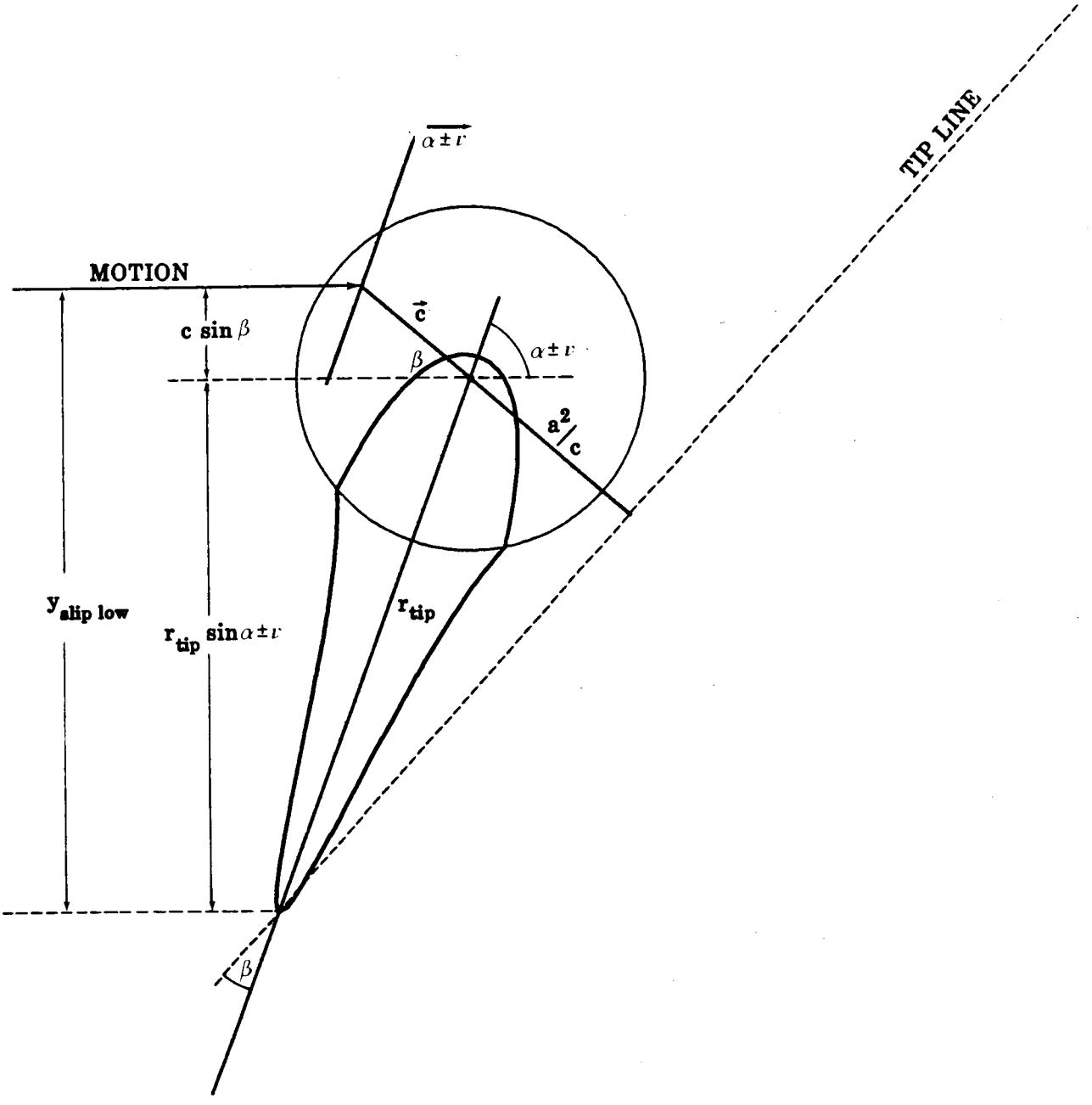

Figure 4-5: COR responsible for slowest rotation in slipping-lowest behavior regime

4.1.2. Sticking-Lowest Behavior

In figure 4-1 the lowest COR is the lowest point of the sticking locus, labeled "B". From figure 4-6 the distance from the line of motion to the lower endpoint of the sticking locus can be approximated as

$$y_{stick\,low} = \frac{c^2 + a^2}{c \sin \beta} \tag{9}$$

Note the absence of any dependence on the friction cone angle ν. This is because when the pusher and object are already sticking, further increase in μ_c has no physical effect. To find the maximum required pushing distance it is only necessary to integrate $dx = y\ d\beta$ with y as given here. We obtain the indefinite integral

$$x = \frac{c^2 + a^2}{2c} \log \left| \frac{1 - \cos \beta}{1 + \cos \beta} \right| \tag{10}$$

In our example, motion from $\beta_{initial} = 45$ degrees until $\beta_{transition} = 69.4$ degrees falls in the sticking-lowest behavior regime, so we simply evaluate x at these two angles and subtract. The distance Δx obtained is the second component of the maximum required pushing distance to align the object. The total required pushing distance to align the object is the sum of the two partial results obtained from equations 8 and 10.

4.2. Correction for the Curvature of the Tip

4.2.1. Slipping-Lowest Behavior

As can be seen from figure 4-7, because of the curvature of the tip of the boundary of the COR locus it is possible for the COR locus to dip slightly below the tip line. The true lowest point is marked 'A', while the point we took to be the lowest in section 4.1.1 is marked 'B'. Using the geometric construction shown in figure 4-7, we can compute a better approximation for the maximum distance from the line of motion to the lowest point of the COR locus (point 'A'):

$$y_{bound} = c \sin \beta + (r_{tip} - s) \sin (\alpha \pm \nu) + s \tag{11}$$

Inserting r_{tip} from equation 1 and the radius of curvature s from equation 2 in equation 11, we find that $dx = y\ d\beta$ cannot be integrated in closed form. However if we make the approximation

$$s = \frac{r_{tip}}{\frac{1}{2} + \frac{r_{tip}^4}{a^4}} \approx \frac{a^4}{r_{tip}^3} \tag{12}$$

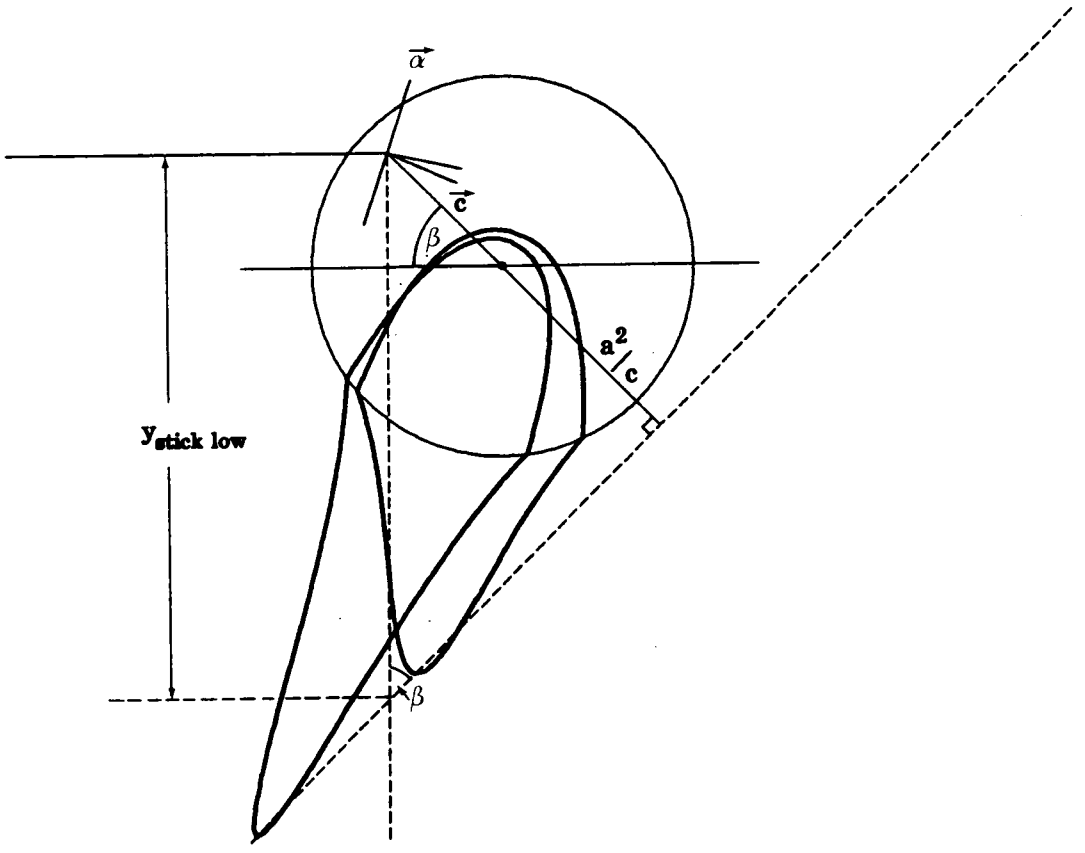

Figure 4-6: COR responsible for slowest rotation in sticking-lowest behavior regime

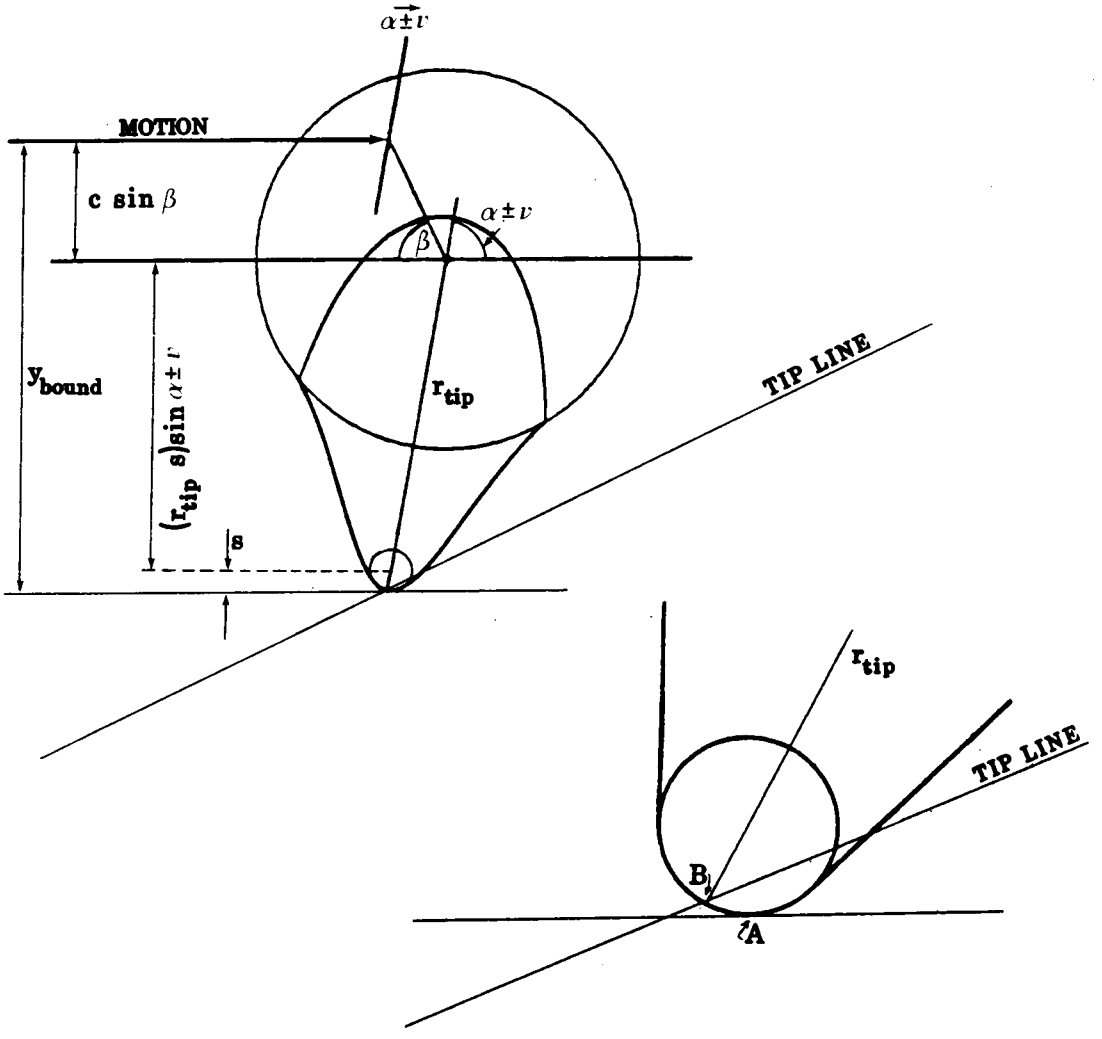

Figure 4-7: Bounding the effect of curvature of the tip, in the slipping-lowest regime

then $dx = y\, d\beta$ can be integrated to yield an indefinite integral representing an additional required pushing distance:

$$x_{adnl} = \frac{-c^3}{a^2}(1 - \sin\alpha\pm\nu)\,(\sin(\alpha\pm\nu+\beta) - \frac{\sin^3(\alpha\pm\nu+\beta)}{3})\,. \tag{13}$$

The approximation made in equation 12 slightly *overestimates* the radius of curvature s, leading to a slight overestimate of y_{bound}, and therefore to a upper bound for the required additional pushing distance x_{adnl}. The sum of equations 8 and 13 provides an upper bound for the required pushing distance. (A slightly lower guaranteed pushing distance could be found.) For practical purposes equation 8 alone will suffice, since the contribution due to tip curvature is small.

4.2.2. Sticking-Lowest Behavior

It is also possible for the lowest point of the sticking locus to fall slightly below the tip line. In figure 4-8 is shown a COR locus $\{COR\}_\alpha$ which intersects the sticking line below the tip line.

If $\{COR\}_\alpha$ has tip curvature s, we find the greatest distance that the curved tip can drop below the tip line to be

$$y_{dip} = \frac{s}{\sin\beta}(1 + \cos(\alpha+\beta)) \tag{14}$$

We do not know the value of α for the locus which produces the lowest point of the sticking locus, but we do know that $r_{tip}(\alpha)$ is greater than the distance (r_x) from the CM to the intersection of the tip line with the sticking line. We evaluate s at radius r_x instead of r_{tip}, and use the angle α_x instead of α in equation 14. The resulting upper bound is:

$$y_{dip} = \frac{\cos^3\alpha_x}{c^3\cos^3\beta\,\sin\beta}(1+\cos(\alpha_x+\beta)) \tag{15}$$

$$\text{where } \tan\alpha_x = \frac{1+c^2+\tan^2\beta}{c^2\tan\beta}$$

Unfortunately $y_{dip}\,d\beta$ cannot be integrated in closed form, and so must be integrated numerically or ignored.

5. Example: Moving Point Pushing Aside a Disk

In this example we consider a disk being pushed not by a fence, but by a point moving in a straight line. The point may be a corner of a polygonal pusher, as long as it is only a corner of the pusher that touches the disk, and not an edge.

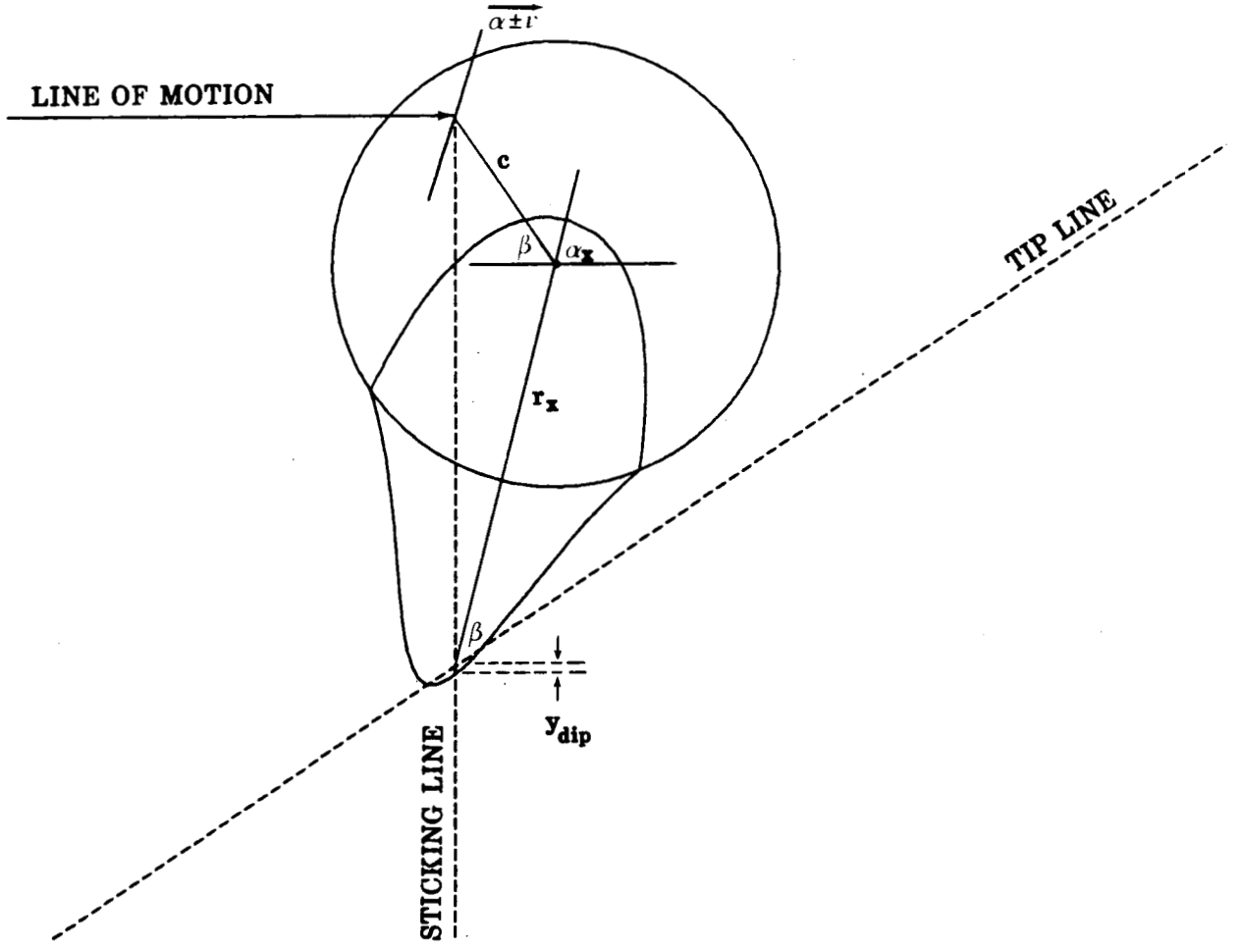

Figure 4-8: Bounding the effect of curvature of the tip, in the sticking-lowest regime

In all cases the outcome of the collision is the same: the disk is pushed aside by the pusher, and contact is broken. The disk ceases to move at the instant the pusher loses contact with it (we assume slow motion), so the disk will be left tangent to the pusher's path when contact is broken. The initial and final configurations of the disk are shown in figure 5-1. We wish to calculate the minimum and maximum length of the encounter, $x_{encounter}$, in terms of the *collision parameter*, β, as indicated in figure 5-1. We might also wish to know the minimum and maximum angles through which the disk may rotate during the collision.

5.1. Length of the Encounter

In figure 5-2, the variables of interest are x, which parametrizes the advance of the pusher along its path, and β, which completely characterizes the collision. β will vary from $\beta_{initial}$, its value at first contact, to $\pi/2$ when contact is broken. $x_{encounter}$ is the corresponding change in x, as β changes from $\beta_{initial}$ to $\pi/2$.

If the instantaneous COR is known, the direction of motion of the CM of the disk is known: it makes an angle θ with the horizontal, as shown in figure 5-2. If the CM of the disk moves a distance Δl along its line of motion, we can find the resulting values of $\Delta\beta$ and Δx, and thereby relate $\Delta\beta$ and Δx to each other.

The pusher advances a distance

$$\Delta x = \Delta l \cos\theta + \Delta l \sin\theta \tan\beta \tag{16}$$

due to Δl. At all times β can be found from

$$a\sin\beta = y + \Delta l \sin\theta \tag{17}$$

where (x,y) are the coordinates of the point of contact.

Substituting Δl from equation 16, and evaluating the change in $\sin\beta$ due to Δl, we find

$$a\Delta(\sin\beta) = \frac{\Delta x \sin\theta}{\cos\theta + \sin\theta\tan\beta} \tag{18}$$

For infinitesimal motions $\Delta\beta$ and Δx become $d\beta$ and dx. Using $d(\sin\beta) = \cos\beta\, d\beta$, we find a differential equation of motion

$$dx = a\, d\beta\,(\sin\beta + \frac{\cos\beta}{\tan\theta}) \tag{19}$$

Since it will turn out that $\tan\theta > 0$, the largest and smallest values of $dx/d\beta$ will result when θ assumes its smallest and largest values, respectively.

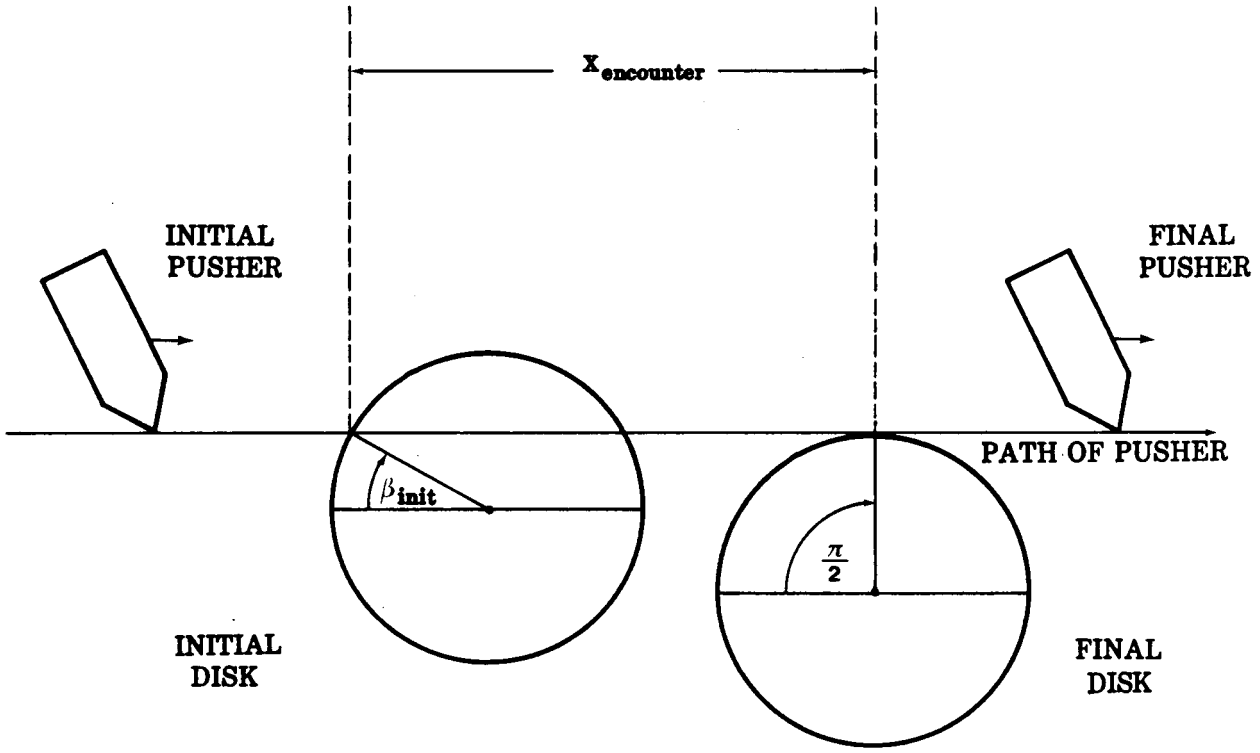

Figure 5-1: Configuration of the disk and the path of the pusher, before and after collision

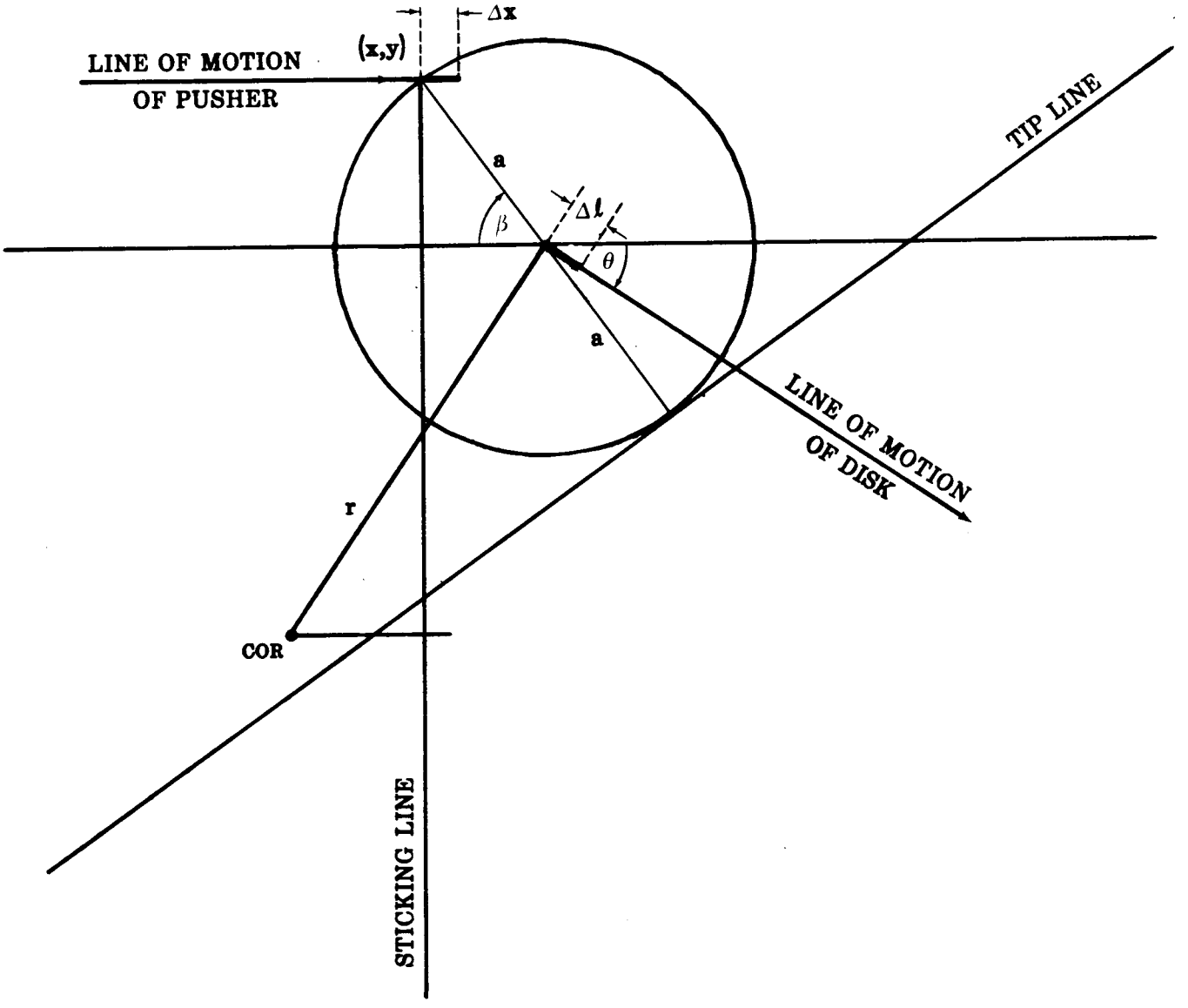

Figure 5-2: Construction for finding the differential equation of motion 16

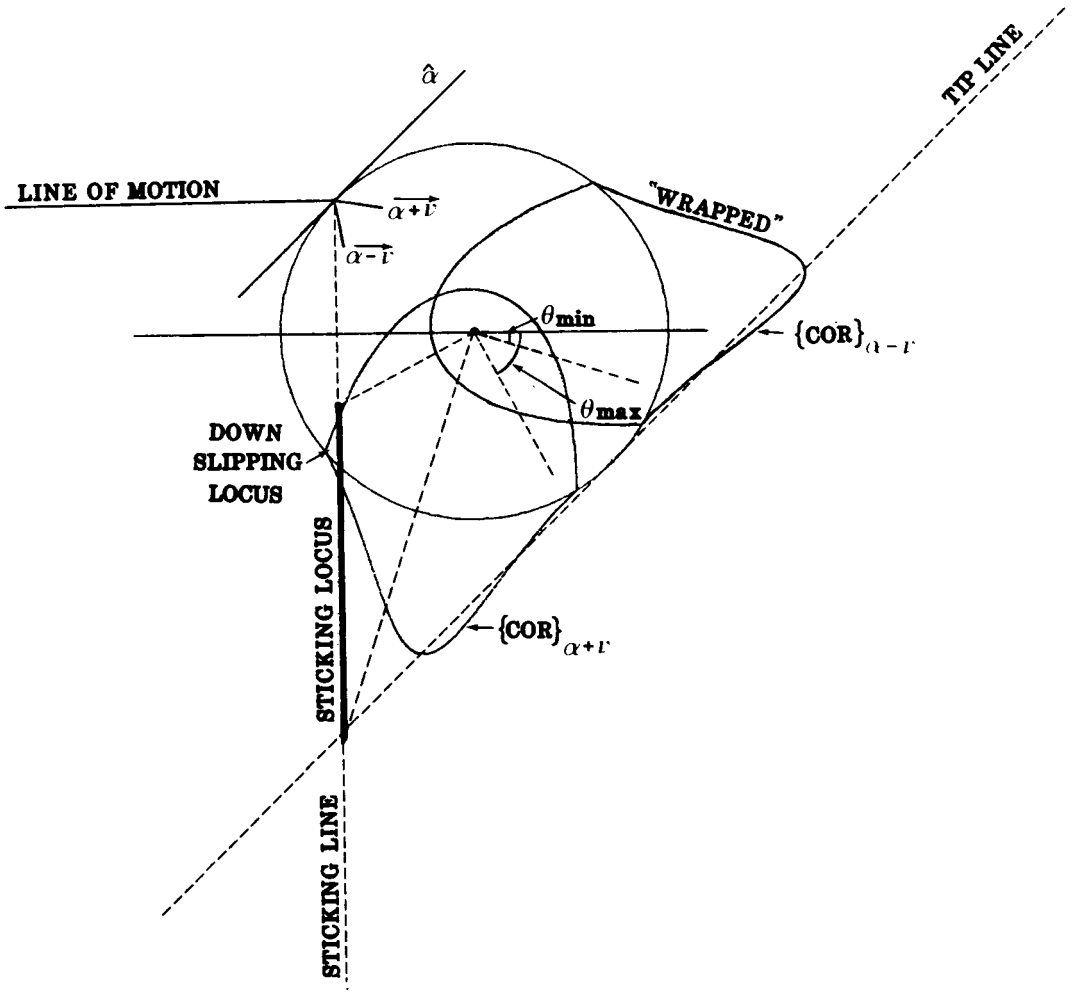

Figure 5-3: COR sketch for a point pushing a disk

Now we construct the COR sketch, shown in figure 5-3. Since the edge normal at $\vec{c}$ passes through the CM, the extremes of the friction cone pass to either side of the CM, for any $\mu_c > 0$. $\{COR\}_{a-p}$ is a "wrapped" locus (as described in section 3.6), so the COR sketch must be that of figure 3-6 sketch (G), (H), or (I). In any case there must be a sticking locus, there cannot be an up-slipping locus, and there may or may not be a down-slipping locus. In figure 5-3 we have shown a down-slipping locus.

In figure 5-3, (and in general when the COR sketch is any one of distinct types (G), (H) or (I)), the smallest and largest values of θ (figure 5-2), occur when the COR is at the lower or upper endpoints, respectively, of the the sticking locus. For sketches (G) and (H) the lower endpoint of the sticking locus is well approximated by the intersection of the sticking line with the tip line, and we will use this approximation (neglecting the small effect of the curvature of the tip, though this could be included). For the lower endpoint of the sticking locus in sketch (I), and for the top of the sticking locus in all three sketches, numerical methods would have to be used. We will not find these numerical results here.

5.1.1. Greatest Length of Encounter

As in section 4.1.2, we will neglect the slight dip of the sticking locus below the tip line, which results from the non-zero radius of curvature of the tip of the COR locus boundary.

We will also assume that the COR sketch is of type (G) or (H), not (I), so that the lower endpoint of the sticking locus can be approximated by the intersection of the sticking line with the tip line. This assumption will be addressed in section 5.1.2, below.

If the COR is at the intersection of the sticking line with the tip line, we find from figure 5-4

$$\tan\theta = \frac{x_{COR}}{y_{COR}} \tag{20}$$

$$x_{COR} = -a\cos\beta, \text{ and}$$

$$y_{COR} = a\frac{\sin^2\beta - 2}{\sin\beta}$$

where y_{COR} is found from the construction of figure 5-4. Using $c = a$, equation 20 can be simplified to

$$\tan\theta = \frac{\cos\beta\sin\beta}{1+\cos^2\beta} \tag{21}$$

Using this value of $\tan\theta$ in the differential equation of motion 19 results in

$$dx = a\,d\beta\,(\sin\beta) + \frac{1+\cos^2\beta}{\sin\beta} \tag{22}$$

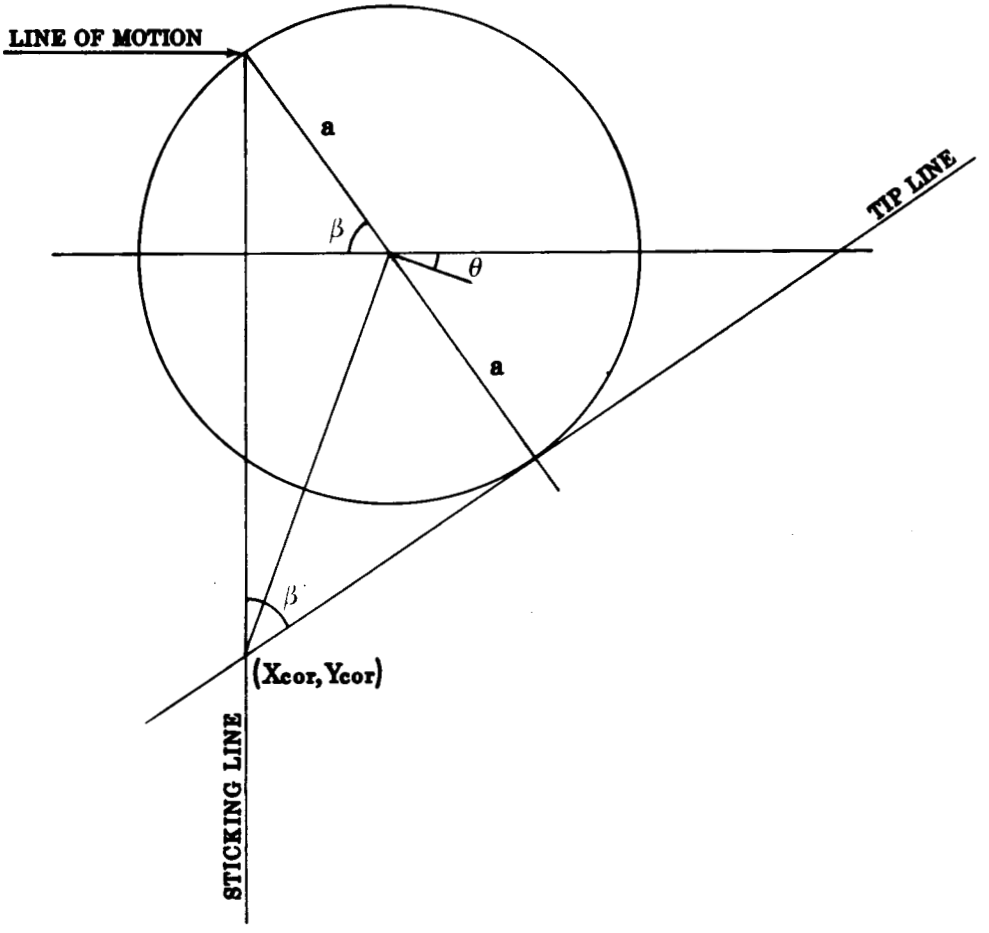

Figure 5-4: Construction for finding the smallest θ (equation 20)

which, integrated, yields the indefinite integral

$$x_{encounter} = a(\ln\frac{1-\cos\beta}{1+\cos\beta}) \tag{23}$$

The maximum value of $x_{encounter}$ can be obtained by evaluating equation 23 at $\beta_{initial}$ and $\pi/2$, and subtracting. The value at $\pi/2$ is zero.

5.1.2. Condition for Sketch Type (I)

The above derivation of maximum $x_{encounter}$ assumed that the lower endpoint of the sticking locus is at the tip line. This is not true when the COR sketch is of type (I), in figure 3-6.

The COR sketch is of type (I) when the tip of $\{COR\}_{\alpha+\nu}$ is left of the sticking line. Simplifying equation 5 for $a = c$ and $\alpha+\beta = \pi/2$, we find the condition for sketch (I) to be:

$$\tan\beta > 2\tan\nu = 2\mu_c \tag{24}$$

This means that the COR sketch will always become type (I) as $\beta \rightarrow \pi/2$, unless $\mu_c = \infty$. ($\mu_c = \infty$ can occur, for example, in pushing a gear, if a tooth is engaged by the pusher.) In every case of pushing aside a disk, sketch (I) is entered eventually.

By using the tip line as the lower endpoint of the sticking locus, despite the fact that this is a poor approximation in sketch (I), we find too low a value for the minimum θ. Our calculated maximum for $x_{encounter}$ (equation 23) is unnecessarily high. We could in principle refine the upper bound by finding the lower endpoint of the sticking locus more accurately by numerical methods.

As mentioned above, we are also neglecting the slight dip of the sticking locus below the tip line (in sketches (G) and (H)), which causes us to underestimate the maximum possible value of $x_{encounter}$. Here too we could refine $x_{encounter}$ by numerical methods, or by using the bound on the dip found in section 4.2.2.

Neglect of sketch (I), and neglect of the dip due to tip curvature, cause errors of opposite sign in calculating the maximum $x_{encounter}$. The latter is a smaller error. Neither error will be addressed here.

5.1.3. Least Length of Encounter

The minimum possible value of $x_{encounter}$ occurs when the COR is at the top of the sticking locus. We do not have an analytical method of finding or approximating the upper endpoint of the sticking locus, as we have for the lower endpoint. The lower endpoint is similarly hard to analyze if the COR sketch is of type (I) in figure 3-6. In these cases it is necessary to find the endpoints numerically for all β in the

range of interest, calculate θ for each β, and then integrate equation 19 numerically to find $x_{encounter}$.

5.2. Rotation of the Pushed Disk during Encounter

5.2.1. Maximum Rotation

In section 5.1, both the largest and smallest possible values of $x_{encounter}$ resulted from CORs on the sticking line. If the COR remains on the sticking line, the pusher does not slip relative to the surface of the disk, and so evaluation of the rotation of the disk during the encounter, $\xi_{encounter}$, is trivial. We have

$$\xi_{encounter} = a(\pi/2 - \beta_{initial}) \tag{25}$$

Since only up-slipping of the pusher is possible, equation 25 is an exact upper bound for $\xi_{encounter}$; any slipping will only serve to reduce the rotation of the disk.

Maximal slipping is obtained if $\mu_c = 0$. The pushing force is directed through the CM of the disk, so the disk can only translate and not rotate [3]. So if $\mu_c = 0$, we have $\xi_{encounter} = 0$ as both maximum and minimum rotation.

5.2.2. Minimum Rotation

We found in section 5.1 that extreme values of $dx/d\beta$ occur when θ takes on extreme values. Having constructed the COR sketch, we found that the extreme values of θ for possible CORs are assumed when the COR falls at the top or bottom of the locus. In this section we will not be able to find a single geometric variable, analogous to θ, whose extremes correspond to extremes of the rate of rotation.

Rotation of the disk will be measured by the angle ξ, measured at the COR, as shown in figure 5-5. We can relate $\Delta\xi$ to advance of the pusher Δx:

$$\Delta x = l\sin\xi \, d\xi \tag{26}$$

Combining equation 26 with equation 19 which relates $\Delta\beta$ to Δx, we find

$$\Delta x = \frac{a\,d\beta\,(\sin\beta + \dfrac{\cos\beta}{\tan\theta})}{l\sin\xi}\, d\beta \tag{27}$$

We can eliminate θ and $l\sin\xi$ in favor of the coordinates of the COR:

$$\tan\theta = \frac{x_{COR}}{y_{COR}} \tag{28}$$

$$l\sin\xi = a\sin\beta - y$$

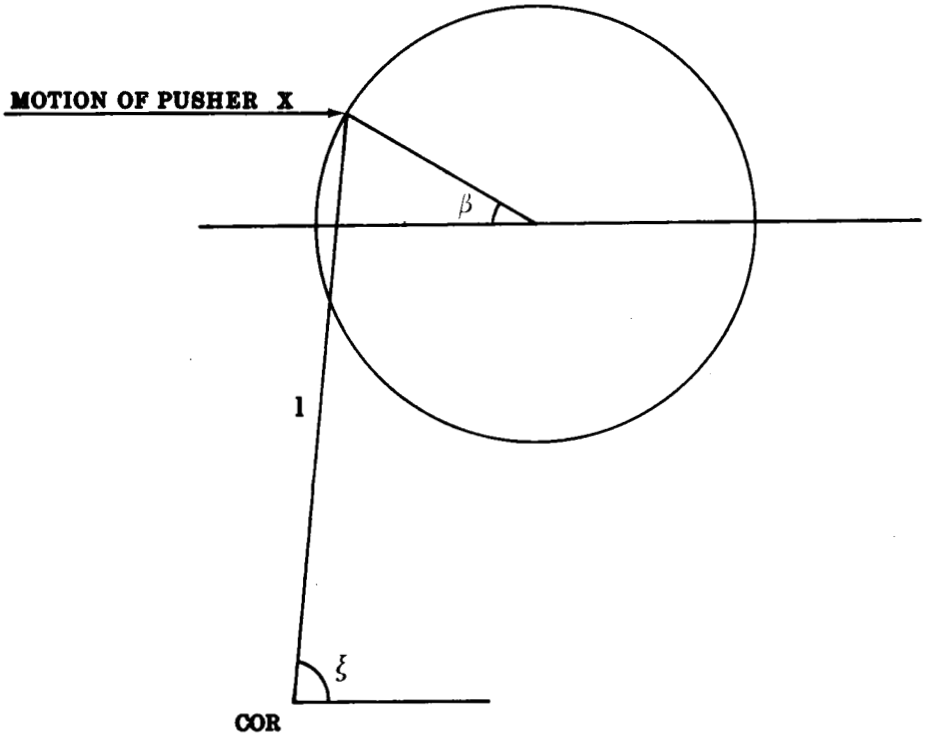

Figure 5-5: Construction for finding the differential equation of motion 26

yielding

$$\frac{d\xi}{d\beta} = \frac{a(y_{COR}\cos\beta + x_{COR}\sin\beta)}{x_{COR}(a\sin\beta - y_{COR})} \tag{29}$$

This has no simple geometric interpretation. Contours of constant $d\xi/d\beta$ are plotted in figure 5-6, for $\beta = 45$ degrees. Minimum rotation occurs at minimum $d\xi/d\beta$. The COR sketch for $\beta = 45$ degrees is superimposed on figure 5-6. The possible value of the COR which is responsible for minimum rate of rotation is the point of the COR locus which intersects the lowest valued contour line, indicated in the figure as point A (in this case very close to the tip). Having obtained numerically the minimum possible value of $d\xi/d\beta$, as a function of β, we can numerically find the indefinite integral:

$$\xi_{min} = \int (\frac{d\xi}{d\beta})_{min}(\beta)\, d\beta \tag{30}$$

Minimum rotation in a given collision can then be evaluated by subtracting $\xi_{min}(\beta_{initial})$ from $\xi_{min}(\pi/2)$.

6. Example: Spiral Localization of a Disk

In this example we analyze an unusual robot motion by which the position of a disk (a washer say), free to slide on a tabletop, can be localized without sensing. If the disk is known initially to be located in some bounded area of radius b_1, we begin by moving a point-like pusher in a circle of radius b_1. Then we reduce the pusher's radius of turning by an amount Δb with each revolution, so that the pusher's motion describes a spiral. Eventually the spiral will intersect the disk (of radius a), bumping it. We wish the disk to be bumped toward the center of the spiral, so that it will be bumped again on the pusher's next revolution. If the spiral is shrinking too fast, however, the disk may be bumped *out* of the spiral instead of toward its center, and so the disk will be lost and not localized.

We wish to find the maximum shrinkage parameter Δb consistent with guaranteeing that the disk is bumped into the spiral, and not out. (Δb will be a function of the present spiral radius.) We also wish to find the number of revolutions that will be required to localize the disk to some radius b, with $a < b < b_1$, and the limiting value of b, called b_∞, below which it will not be possible to guarantee localization, regardless of number of revolutions.

6.1. Analysis

Suppose the pushing point has just made contact with the disk. Since the previous revolution had radius only Δb greater than the current revolution, the pusher must contact the disk at a distance at most Δb from the edge of the disk, as shown in figure 6-1. We will consider only the worst case, where the distance of the pusher from the edge is the full Δb.

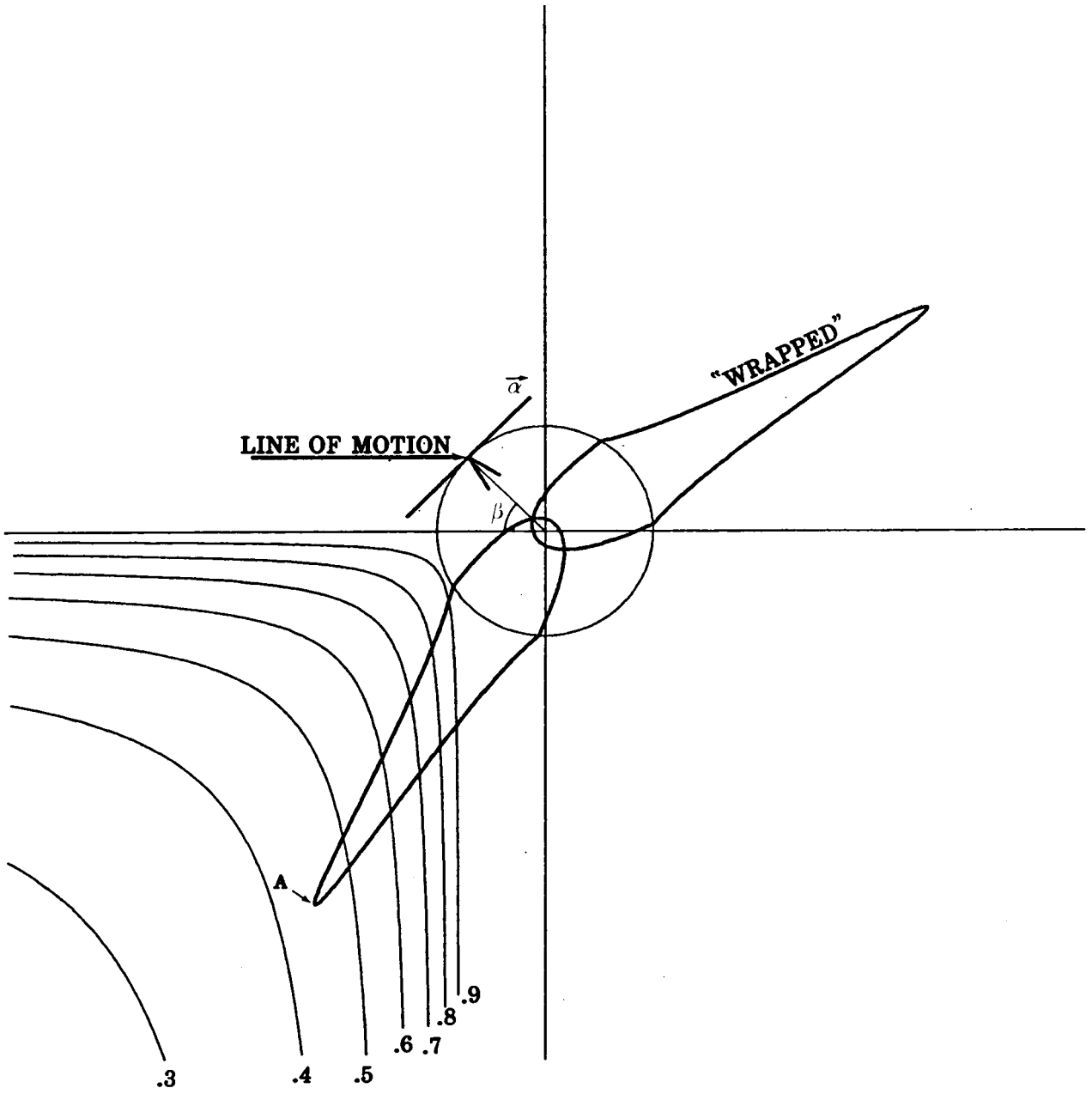

Figure 5-6: Contours of constant $d\xi/d\beta$, and the COR sketch

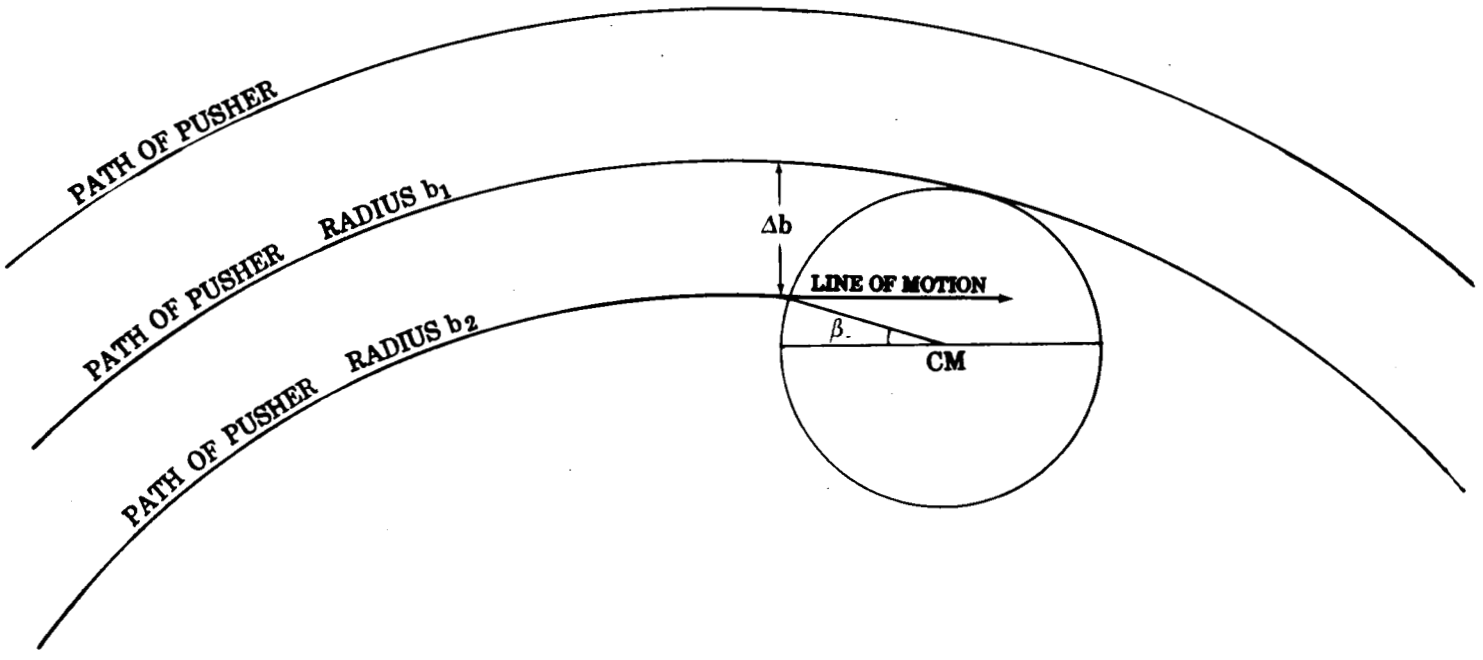

Figure 6-1: Geometry at the moment of the second collision of pusher and disk

We know that if $\Delta b < a$ the disk will move downward [3]. This is not sufficient to assure that the disk will be pushed into the spiral (rather than out of the spiral), because the pushing point will also move down, as it continues along its path (figure 6-1). To guarantee that the disk will be pushed into the spiral, we must make sure that it moves down *faster* than does the pushing point.

Note that we will continue to draw the pusher's motion as horizontal, even though the pusher must turn as it follows the spiral. This is done to maintain the convention for COR sketches used in previous sections. At every moment we simply choose to view the system from such an angle that the pusher's motion is horizontal.

One way of comparing rates of moving down is by considering the increase or decrease in the angle β, called the *collision parameter*, in figure 6-1. If, as the pusher's motion along its spiral progresses, β increases, then the disk is being pushed *into* the spiral; localization is succeeding. When β reaches $\pi/2$, the pusher grazes the disk and leaves it behind. The disk is then left tangent to the spiral. If, as the pusher's motion progresses, β decreases, the disk is being pushed *out* of the spiral; localization is failing.

6.2. Critical Case: Pusher Chasing the Disk around a Circular Path

In the critical case the angle β does not change with advance of the pusher. The pusher "chases" the disk around the spiral, neither pushing it in nor out. In this section we will take the spiral to be a circle (i.e., $\Delta b = 0$), to simplify analysis. The critical case, shown in figure 6-2, is highly unstable. The pusher's motion is shown as an arc of a circle, labeled path of pusher. (Underlined names refer to elements of figure 6-2). The center of that circle is labeled PC (for pusher-center). Point PC is directly below the point of contact, in keeping with our convention of drawing the pusher's line of motion horizontal.

To maintain the critical case, the path followed by the CM of the disk (labeled critical path of CM) must be as shown in the figure: an arc of a circle, concentric with the arc path of pusher. Instantaneously, the direction of motion of the CM must be along the line labeled motion of CM, tangent to the critical path of CM. The critical line, drawn through PC and CM, is by construction perpendicular to motion of CM. The COR of the disk must fall on the critical line, in order that the instantaneous motion along the line motion of CM be tangent to the critical path of CM.

We have just seen that the COR of the disk must fall on critical line for the instantaneous motion of the CM to be consistent with the CM following the critical path of CM. If the COR falls to the left of the critical line, the CM diverges from the critical path of CM by moving *inside* the arc. Therefore β will

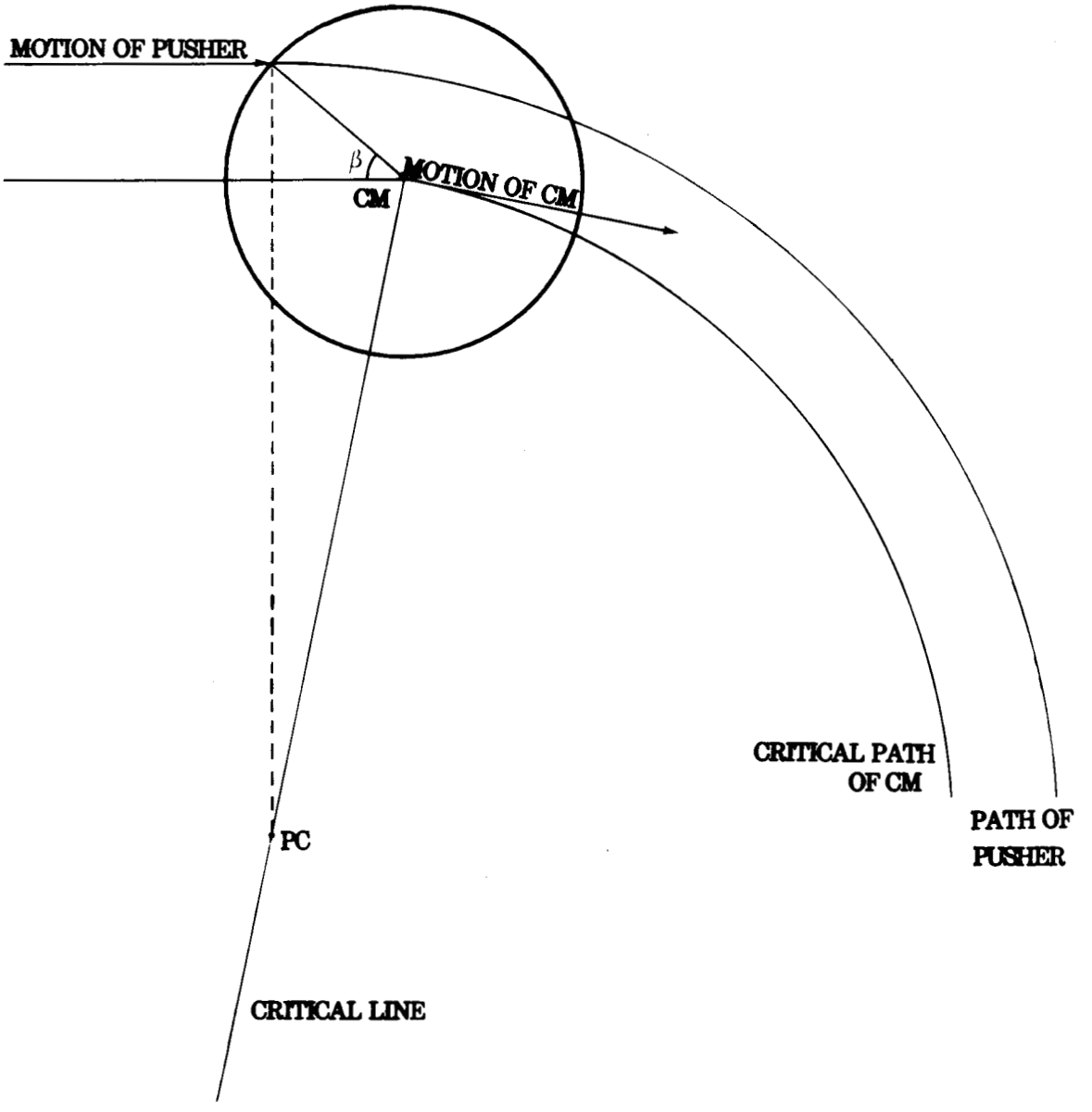

Figure 6-2: Critical case: pusher "chasing" disk around a circular path

increase with advance of the pusher, and localization is succeeding. If the COR falls to the right of the critical line, the CM diverges from the critical path of CM by moving *outside* the arc. Therefore β will decrease with advance of the pusher, and localization is failing. The critical line divides the plane into two zones: if the COR falls in the left zone, the disk is pushed into the pusher circle, while if the COR falls in the right zone, the disk is pushed out of the pusher circle.

We wish to find a condition on the radius of the pusher circle which guarantees that the disk will always be pushed *into* the circle. We will construct the COR sketch, and then find positions for PC such that all possible CORs are to the left of the critical line.

In figure 6-3 we have constructed the COR sketch with collision parameter β. Since the edge normal at $\vec{c}$ passes through the CM, the extremes of the friction cone pass to either side of the CM, for any $\mu_c > 0$. $\{COR\}_{\alpha-\nu}$ is a "wrapped" locus (section 3.6), and the COR sketch must be that of figure 3-6 (G), (H), or (I). In any case, there must be a sticking locus, there cannot be an up-slipping locus, and there may or may not be a down-slipping locus. In figure 6-3 we have shown a down-slipping locus.

To make sure that the whole COR locus falls to the left of critical line, we need only place the center of the pusher motion (PC) *below* the lower endpoint of the sticking locus. (Point PC is required to have the same x coordinate as the point of contact, in keeping with our convention of drawing the pusher's line of motion horizontal.)

6.3. Critical Radius vs. Collision Parameter

For every value of β, (the collision parameter), we compute the distance from the pusher's line of motion to the lower endpoint of the sticking locus. This defines a critical radius $r^*(\beta)$. For each collision parameter β, $r^*(\beta)$ is the radius the tightest circle that the pusher can describe with the guarantee that the disk will be pushed into the circle, or at worst be "chased" around the circle indefinitely, but not be pushed out of the circle. In figure 6-4, $1/r^*(\beta)$ is plotted as a function of collision parameter β for each of several values of μ_c. (The discontinuity in slope results from the discontinuity in slope of the COR locus boundary at $r = a$.)

The inverse of the function $r^*(\beta)$ will be denoted $\beta^*(r)$, representing the smallest value of β for which a pusher motion of radius r still results in guaranteed localization. In terms of the pusher's distance from the top edge of the disk, d, (figure 6-3), we can use the relationship

$$a(1 - \sin\beta) = d \tag{31}$$

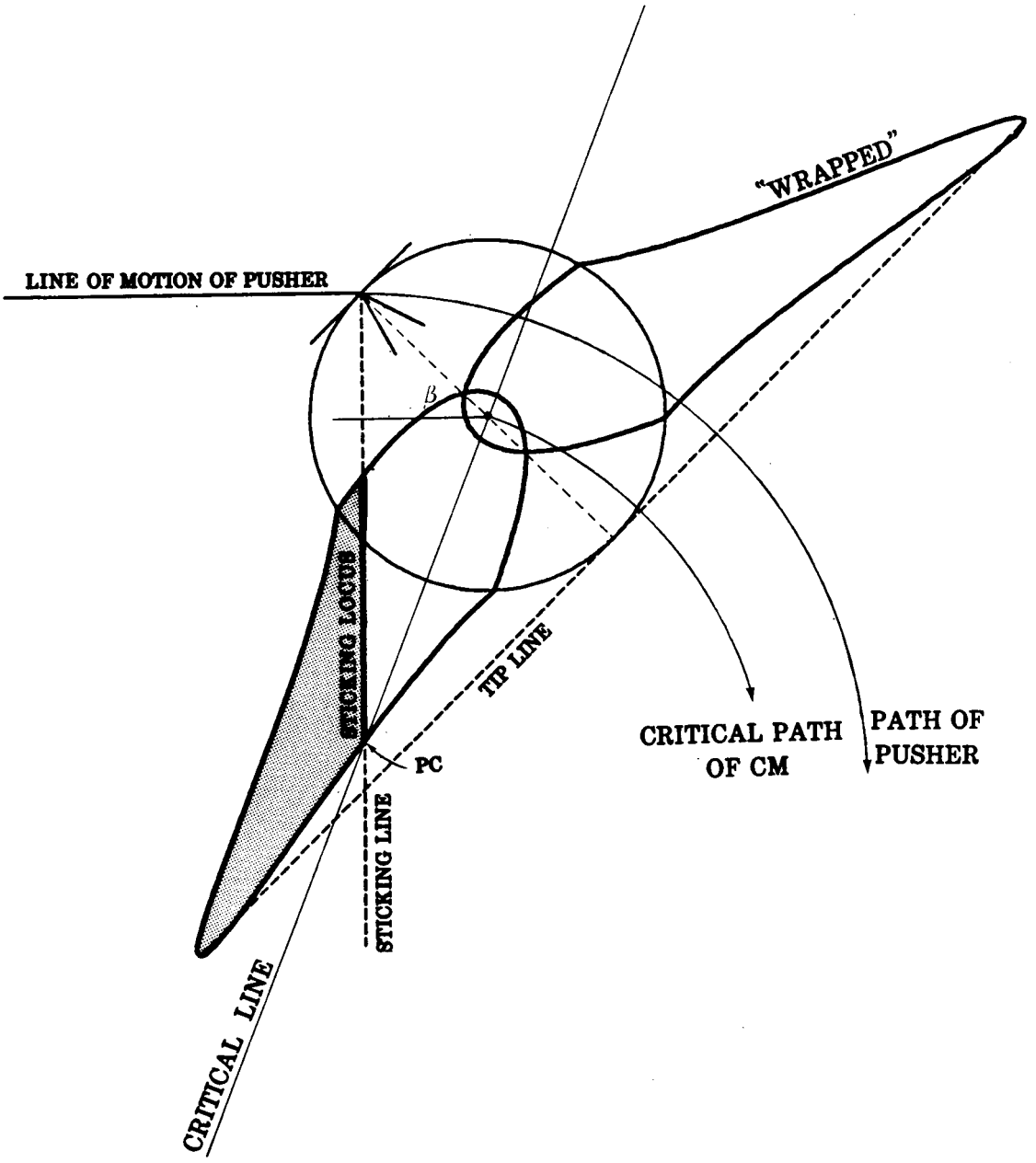

Figure 6-3: COR sketch for critical case, and solution for location of PC

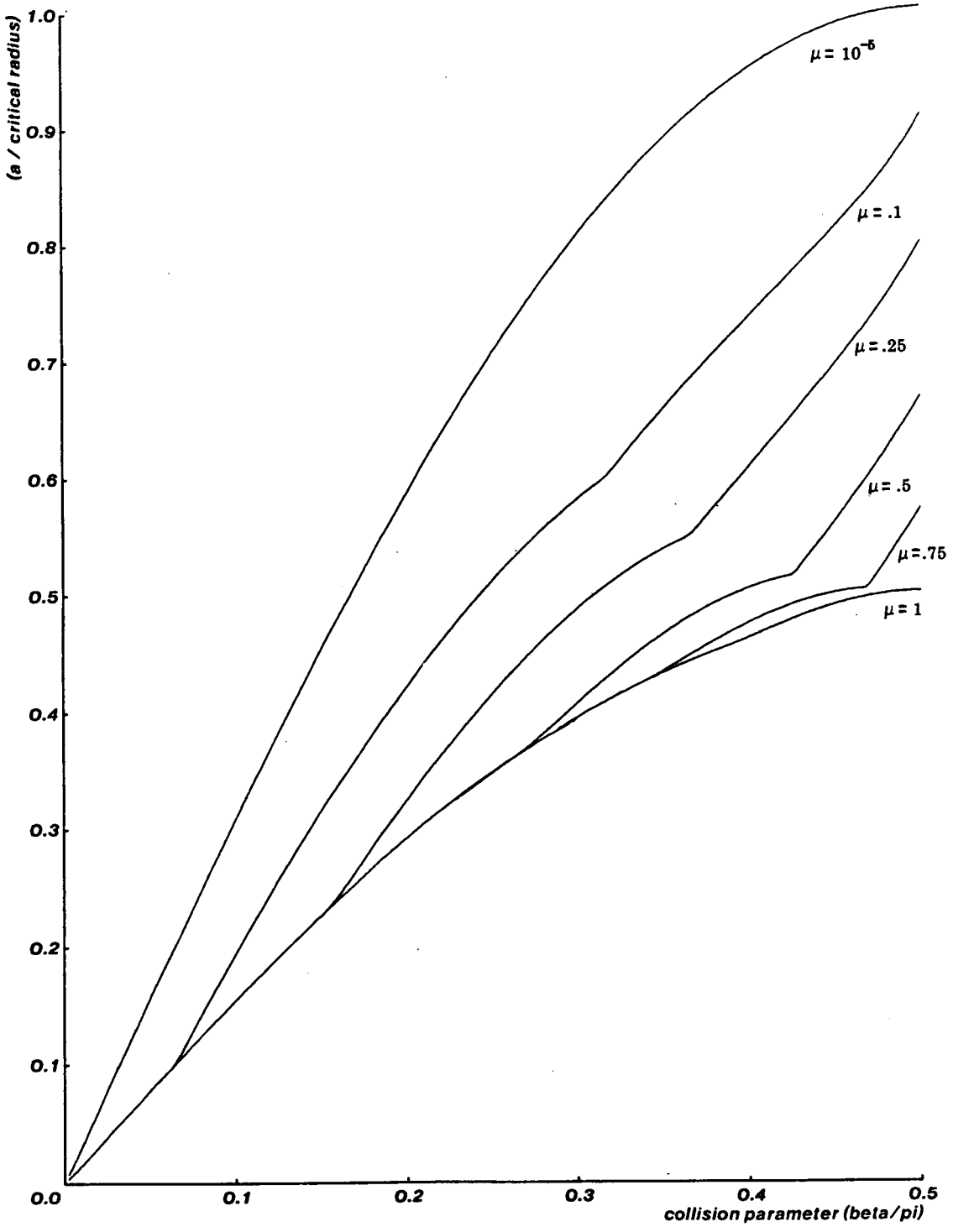

Figure 6-4: Radius $r^*(\beta)$ of the critical circle as a function of collision parameter β

to define the *critical distance from grazing* $d^*(r)$ as a function of r. $d^*(r)$ is the largest distance of the pusher from the top edge of the disk for which a pusher motion of radius r still results in guaranteed localization.

6.4. Limiting Radius for Localization

If there is a limiting radius b_∞ of the spiral motion below which localization cannot be guaranteed, then as the spiral approaches radius b_∞ the motion must become circular. $\Delta b \to 0$ as b_∞ is approached, so collisions become grazing collisions, and we have the distance from grazing $d \to 0$. (In terms of the collision parameter β, we have $\beta \to \pi/2$.) The COR sketch for $\beta = \pi/2$ is shown in figure 6-5. If the disk is not to be bumped out of the spiral, we must have $b_\infty = r^*(\beta = \pi/2)$. b_∞ is indicated in the figure, and can be shown analytically to be

$$b_\infty = a(\mu_c + 1) \text{ for } \mu_c \le 1 \qquad (32)$$

$$b_\infty = 2a \text{ for } \mu_c \ge 1$$

Only at $\mu_c = 0$ can a disk be localized completely, i.e. localized to within a circle the same radius as the disk. Otherwise the tightest circle within which the disk can be localized is given by equation 32.

6.5. Computing the Fastest Guaranteed Spiral

Let b_n be the radius of the n^{th} revolution of the pusher, so that we have initially radius b_1, and b_∞ is the limiting radius as $n \to \infty$ (In specifying but a single radius for each revolution of the spiral, we will not truly specify the spiral completely, but this will be sufficient to characterize the number of revolutions required to achieve a desired degree of localization.)

We will define two spirals recursively, in terms of b_n. The first of these will be "too-fast": the spiral described shrinks so fast that it is possible for the disk to be pushed out of the spiral. The second will be "too-slow": the spiral described will guarantee localization, but will not be the fastest spiral to do so. The "too-fast" and "too-slow" spirals will differ very little, and so will place tight bounds on the performance of the exact fastest guaranteed spiral.

6.5.1. Too-Fast Spiral

The too-fast spiral is defined recursively by

$$b_n = b_{n-1} - d^*(b_n) \qquad (33)$$

The difference between the radii of consecutive turns of the spiral $n-1$ and n, is therefore

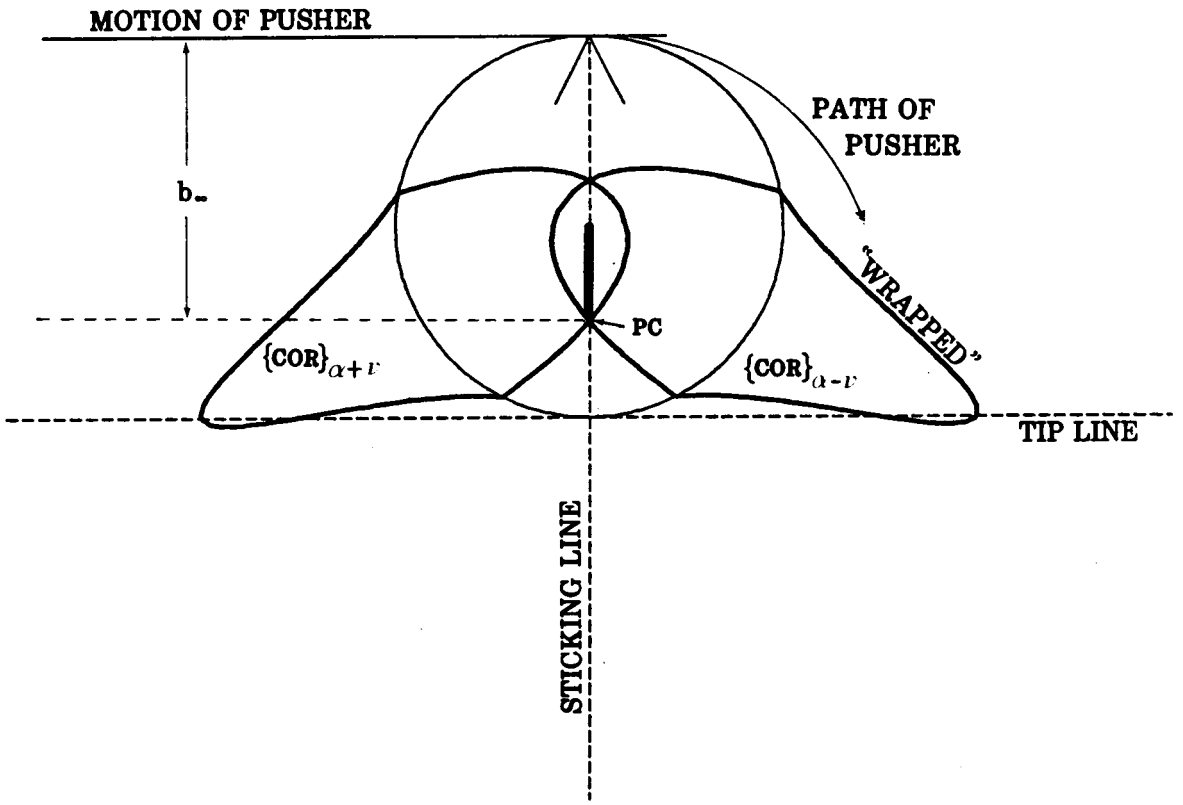

Figure 6-5: COR sketch at the limiting radius, showing b_∞

$\Delta b = d^*(b_n)$. Equation 33 thus enforces the condition that on the n^{th} revolution, the value of d is exactly the critical value for circular pushing motion of radius b_n. At worst, the disk is pushed neither in nor out of the spiral. Unfortunately the spiral radius is b_n only for an instant, and then decreases. It is then possible for the disk to be pushed out of the spiral. The spiral described by equation 33 does not guarantee localization.

6.5.2. Too-Slow Spiral

Consider the spiral defined by

$$b_n = b_{n-1} - d^*(b_{n+1}) \tag{34}$$

The difference between the radii of consecutive turns of the spiral $n-1$ and n, is $\Delta b = d^*(b_{n+1})$. Equation 34 enforces the condition that on the n^{th} revolution, the value of d is exactly the critical value for circular pushing motion of radius b_{n+1}. Here the value of d on the n^{th} revolution is the critical one, not for radius b_n as above, but for b_{n+1}. At the beginning of the n^{th} revolution, the value of the d is such that it is guaranteed that the disk be pushed into the spiral. The radius of the spiral remains *above* the critical radius for d for an entire revolution (until revolution $n+1$). We need only show that the disk cannot be "chased" for an entire revolution in this condition; it will first be bumped into the spiral and lose contact with the pusher.

In figure 6-6 are shown the path of the pusher during the first half of revolution n, and also the tightest path the pusher could take with the guarantee that, at worst, the disk would be "chased" and not pushed out of the spiral. The initial position of the disk is shown at the top, common to both proposed paths of the pusher. At the bottom is shown the worst case final position of the disk, if the pusher takes the tighter path. Since this final position places the disk entirely within the looser proposed path, we know that if the pusher takes the looser path it must loose contact with the disk before the pusher has executed half of a revolution.

6.5.3. Performance of the Two Spirals

Figure 6-7 shows the fractional deviation of spiral radius b_n above b_∞, vs. number of turns n, on logarithmic and on linear scales. In both the "too-fast" and the "too-slow" spirals we start (arbitrarily) with $b_1 = 100\,a$. The spiral radii were computed numerically for $\mu_c = .25$, using the results for $\beta^*(r)$ shown in figure 6-4, and equations 33 or 34. Since the optimal spiral must fall between the "too-fast" and the "too-slow" spirals, we have very tight bound on the optimal spiral.

Figure 6-7 shows that when the spiral radius is large compared to the disk radius a (which is taken to

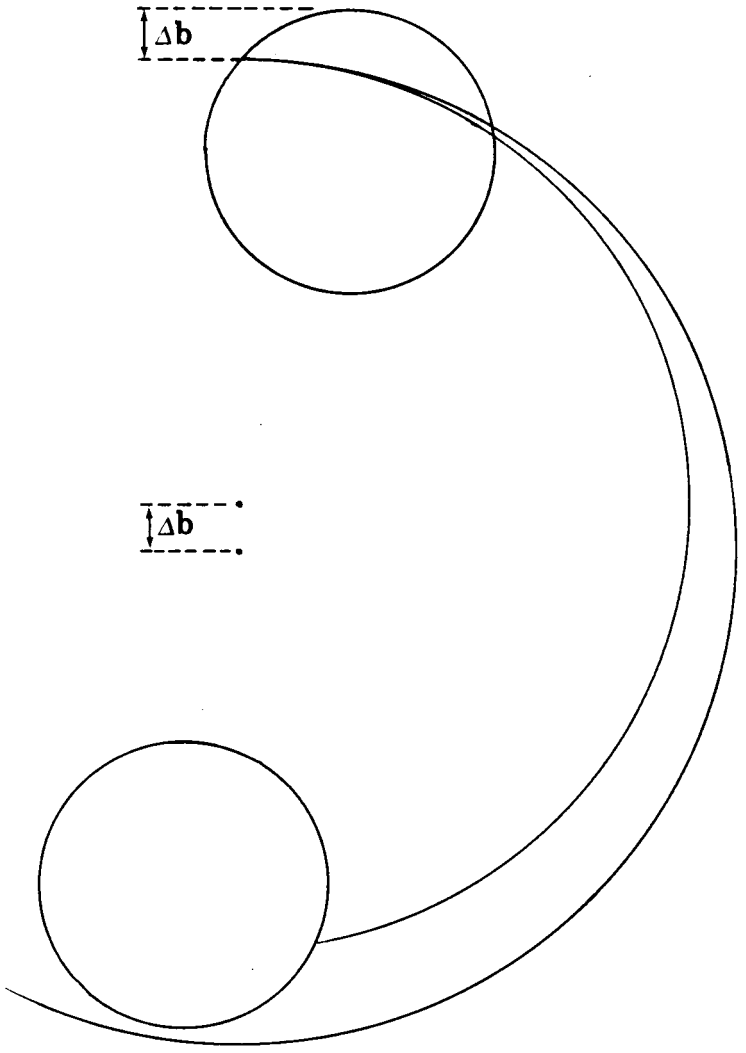

Figure 6-6: Construction showing why "too-slow" spiral is guaranteed to localize the disk

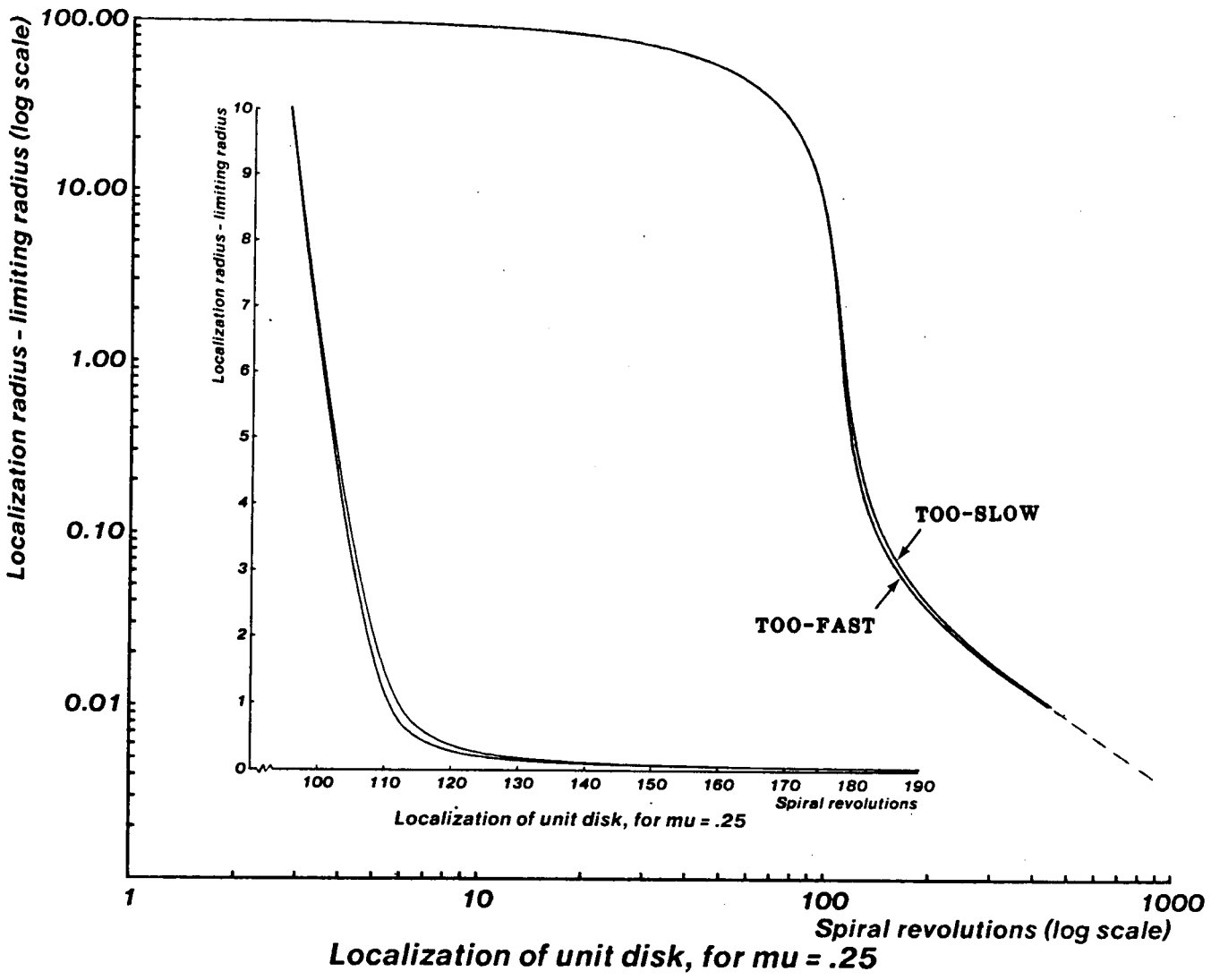

Figure 6-7: Performance of "too-slow" and "too-fast" spirals

be 1 in the figure), we can reduce the radius of the spiral by almost a with each revolution. As the limiting radius is approached, the spiral reduces its radius more and more slowly, approaching the limiting radius b_∞ as about $n^{-1.6}$, where n is the number of revolutions.

Figure 6-7 demonstrates the best performance that the "herding" strategy can acheive.

7. Conclusion

We have shown how bounds can be placed on the possible instantaneous motions of a sliding object being pushed by another object, in the presence of unknown frictional forces between object and table, and between object and pusher. We have characterized the qualitatively different kinds of sliding motion which are possible, and found the conditions under which each can occur.

Using these results it is possible to find bounds for *gross* motions of a pushed object as well. This is done by integrating the possible instantaneous motions.

As an example, we have found the maximum distance a polygonal sliding object must be pushed by a fence in order to guarantee that a side of the object has aligned itself with the fence. This is the same problem considered in [4], but here we have included a non-zero coefficient of friction between the polygon and the pusher. Using the useful *tip line construction* described here, approximate results are obtained both for the alignment problem and several others. Strict upper bounds for the maximum required pushing distance are found by using slightly more sophisticated methods, but the difference between the upper bounds and the approximate results are so slight that the effort seems hardly justified.

In a second example, we have taken the pushed object to be a disk, and the pusher to be a point, or the corner of a polygon, moving in a straight line. We have found the maximum disatnce that the pusher and the disk may be in contact, before the disk is "pushed aside" by the moving object. Bounds on the rotation of the disk during its interaction with the pusher are also found.

Finally we have analysed an unusual robot manuever, in which a disk known to be within a certain circular area can be "localized" to a much smaller circular area by a pusher which, perhaps under robot control, describes a decreasing spiral around the disk. Thus the disk can be located by a robot without sensors. We found the ultimate limiting radius below which the disk cannot be localized further, no matter how slowly the spiral decreases in radius. We also found (to within tight bounds) the "optimal spiral": the spiral which localizes the disk with the fewest number of revolutions, while guaranteeing that the disk is not lost from the spiral.

We believe that the motion of a sliding object is now sufficiently well understood that reliable robot strategies taking advantage of sliding motion can be designed and verified. Brost [1] and Mani [2] have independently developed graphical methods for description of sliding motion, based on the results of Mason [3].

The above mentioned work (including our work) has the limitation of assuming slow (quasistatic) motion of pushed objects. In the opposite limit, fast motion, friction between the pushed object and the table can be ignored. If the coefficient of friction between pusher and pushed object is known, the motion of the pushed object can be solved exactly (rather than bounded as we have done here.) This problem is presently under study by several workers. It will be necessary to solve the intermediate case, or at least to bound the effects of inertia, in order to deal with other than quasistatic motions.

The bounds on possible motions described in our work are exact bounds only when the sliding object is a disk. For other objects, tighter bounds exist. If the bounds for a disk are used in constructing a strategy for manipulating an object much smaller than its circumscribed disk (for instance a thin rectangle), unduly conservative strategies may result.

8. Acknowledgements

We wish to acknowledge useful discussions with Randy Brost and with Matt Mason. We thank Jeff Koechling for a careful reading of this paper.

References

1. Brost, Randy. Planning Robot Grasping Motions in the Presence of Uncertainty. CMU-RI-TR-85-12, Carnegie-Mellon University, 1985.

2. Mani, Murali and W.R.D. Wilson. A Programmable Orienting System for Flat Parts. , NAMRII XIII, 1985.

3. Mason, Matthew T., J. K. Salisbury. *Robot Hands and the Mechanics of Manipulation.* The MIT Press, 1985.

4. Peshkin, M. A. and A. C. Sanderson. The Motion of a Pushed, Sliding Object (Part 1: Sliding Friction). CMU-RI-TR-85-18, Robotics Institute, Carnegie-Mellon University, 1985.